

The University of British Columbia

FACULTY OF GRADUATE STUDIES

PROGRAMME OF THE
FINAL ORAL EXAMINATION
FOR THE DEGREE OF
DOCTOR OF PHILOSOPHY

of

WARREN DAVID LITTLE

B.A.Sc., The University of British Columbia, 1961

M.A.Sc., The University of British Columbia, 1963

FRIDAY, OCTOBER 22, 1965, at 4:00 P.M.
IN ROOM 402, MacLEOD BUILDING

COMMITTEE IN CHARGE

Chairman: I. McT. Cowan

E. V. Bohn

A. D. Moore

R. W. Donaldson

C. A. Swanson

H. P. Zeiger

Research Supervisor: A. D. Soudack

External Examiner: L. D. Kovach

Pepperdine College
Los Angeles, California

HYBRID COMPUTER SOLUTIONS OF PARTIAL DIFFERENTIAL
EQUATIONS BY MONTE CARLO METHODS

ABSTRACT

A continuous Markov process is examined for the purpose of developing Monte Carlo methods for solving partial differential equations. Backward Kolmogorov equations for conditional probability density functions and more general equations satisfied by auxiliary probability density functions are derived. From these equations and the initial and boundary conditions that the density functions satisfy, it is shown that solutions of partial differential equations at an interior point of a region can be written as the expected value of randomly-selected initial and boundary values. From these results, Monte Carlo methods for solving homogeneous and nonhomogeneous elliptic, and homogeneous parabolic partial differential equations are proposed.

Hybrid computer techniques for mechanizing the Monte Carlo methods are given. The Markov process is simulated on the analog computer and the digital computer is used to control the analog computer and to form the required averages. Methods for detecting the boundaries of regions using analog function generators and electronic comparators are proposed.

Monte Carlo solutions are obtained on a hybrid system consisting of a PACE 231 R-V analog computer and an ALWAC III-E digital computer. The interface for the two computers and a multichannel discrete-interval binary-noise source are described. With this equipment, solutions having a small variance are obtained at a rate of approximately five minutes per solution. Example

solutions are given for Laplace's equation in two and three dimensions, Poisson's equation in two dimensions and the heat equation in one, two and three dimensions.

GRADUATE STUDIES

Field of Study: Electrical Engineering

Applied Electromagnetic Theory	G. B. Walker
Electronic Instrumentation	F. K. Bowers
Network Theory	A. D. Moore
Servomechanisms	E. V. Bohn
Solid-State Electronic Devices	M. P. Beddoes
Nonlinear Systems	A. C. Soudack
Electron Dynamics	G. B. Walker
Digital Computers	E. V. Bohn

Related Studies:

Numerical Analysis I	T. Hull
Computer Programming	C. Froese
Integral Equations	E. Macskasy

PUBLICATIONS

Beddoes, M.P. and Little, W.D., "Unilateral Parametric Frequency Converters with Nonlinear Conductance and Capacitance", Proc. IEEE, Vol. 52, No. 3, p. 333, March, 1964.

Soudack, A.C. and Little, W.D., "An Economical Hybridizing Scheme for Applying Monte Carlo Methods to the Solution of Partial Differential Equations", Simulation, Vol 5, No. 1, pp. 9-11, July, 1965.

Little, W.D., "An Electronic SPDT Switch", Simulation, Vol. 5, No. 1, P. 12, July, 1965

Little, W.D., and Soudack, A.C., "On the Analog Computer Solution of First-Order Partial Differential Equations", Annales AsICA, October, 1965.

Kohne, H., Little, W.D., and Soudack, A.C., "An Economical Multichannel Noise Source", Simulation, to be published, November, 1965.

HYBRID COMPUTER SOLUTIONS OF PARTIAL
DIFFERENTIAL EQUATIONS BY MONTE CARLO METHODS

by

WARREN DAVID LITTLE

B.A.Sc., University of British Columbia, 1961

M.A.Sc., University of British Columbia, 1963

A THESIS SUBMITTED IN PARTIAL FULFILMENT OF
THE REQUIREMENTS FOR THE DEGREE OF

DOCTOR OF PHILOSOPHY

in the Department of
Electrical Engineering

We accept this thesis as conforming to the
required standard

Members of the Department
of Electrical Engineering
THE UNIVERSITY OF BRITISH COLUMBIA

October, 1965

In presenting this thesis in partial fulfilment of the requirements for an advanced degree at the University of British Columbia, I agree that the Library shall make it freely available for reference and study. I further agree that permission for extensive copying of this thesis for scholarly purposes may be granted by the Head of my Department or by his representatives. It is understood that copying or publication of this thesis for financial gain shall not be allowed without my written permission.

Department of Electrical Eng.
The University of British Columbia
Vancouver 8, Canada
Date Oct 25/65

ABSTRACT

A continuous Markov process is examined for the purpose of developing Monte Carlo methods for solving partial differential equations. Backward Kolmogorov equations for conditional probability density functions and more general equations satisfied by auxiliary probability density functions are derived. From these equations and the initial and boundary conditions that the density functions satisfy, it is shown that solutions of partial differential equations at an interior point of a region can be written as the expected value of randomly-selected initial and boundary values. From these results, Monte Carlo methods for solving homogeneous and nonhomogeneous elliptic, and homogeneous parabolic partial differential equations are proposed.

Hybrid computer techniques for mechanizing the Monte Carlo methods are given. The Markov process is simulated on the analog computer and the digital computer is used to control the analog computer and to form the required averages. Methods for detecting the boundaries of regions using analog function generators and electronic comparators are proposed.

Monte Carlo solutions are obtained on a hybrid system consisting of a PACE 231 R-V analog computer and an ALWAC III-E digital computer. The interface for the two computers and a multichannel discrete-interval binary-noise source are described. With this equipment, solutions having a small variance are obtained at a rate of approximately five minutes per solution. Example solutions are given for Laplace's equation in two and three dimensions, Poisson's equation in two dimensions and the heat equation in one, two and three dimensions.

TABLE OF CONTENTS

	Page
List of Illustrations	vi
Acknowledgements	viii
1. INTRODUCTION	1
1.1 Introduction	1
1.2 Thesis Outline	4
2. FUNDAMENTAL RELATIONS FOR MARKOV PROCESSES	5
2.1 Introduction	5
2.2 Chapman-Kolmogorov Equations for Continuous Markov Processes within Bounded Regions	5
2.3 Backward Kolmogorov Partial Differential Equations	10
2.4 A Continuous Markov Process for which Backward Kolmogorov Equations are Valid	17
2.5 Partial Differential Equations Satisfied by Auxiliary Probability Density Functions	23
3. MONTE CARLO METHODS FOR THE SOLUTIONS OF BOUNDARY- VALUE PROBLEMS.....	30
3.1 Introduction	30
3.2 Solutions of Boundary-Value Problems for Parabolic Partial Differential Equations	31
3.3 Solutions of Boundary-Value Problems for Elliptic Partial Differential Equations	39
3.4 Solutions of Nonhomogeneous Boundary-Value Problems	42
3.5 Estimates of the Number of Random Walks for Monte Carlo Solutions	45
3.5A Convergence of Monte Carlo Solutions	45
3.5B Number of Random Walks for Homogeneous Partial Differential Equations	46
3.5C Number of Random Walks for Nonhomogeneous Partial Differential Equations	47

	Page
4. COMPUTER MECHANIZATION OF MONTE CARLO METHODS FOR SOLVING PARTIAL DIFFERENTIAL EQUATIONS	50
4.1 Introduction	50
4.2 Simulation of the Stochastic Process on an Analog Computer	52
4.2A Analog Computer Setup	52
4.2B Noise Source Requirements	55
4.2C Effect of Finite Bandwidths on Solution Times	56
4.3 Detection of Boundaries	57
4.3A Detection of Boundaries for Problems with One Space Variable	60
4.3B Detection of Boundaries for Problems with Two Space Variables	61
4.3C Detection of Boundaries for Problems with Three Space Variables	66
4.4 Generation of Initial and Boundary Values	67
4.5 Operations Performed by the Digital Computer ..	69
5. HYBRID COMPUTER SOLUTIONS OF ILLUSTRATIVE PROBLEMS .	73
5.1 Introduction	73
5.2 One-Dimensional Boundary-Value Problems	73
5.3 Laplace's Equation in Two Dimensions	79
5.4 Poisson's Equation in Two Dimensions	79
5.5 Heat Equation in One, Two and Three Dimensions.	84
5.6 Laplace's Equation in Three Dimensions	86
5.7 Discussion of Results	86
6. CONCLUSIONS	89

	Page
APPENDIX I	
INTERFACE FOR TRANSFER OF DATA BETWEEN THE PACE 231 R-V AND THE ALWAC III-E	91
APPENDIX II	
MULTICHANNEL DISCRETE-INTERVAL BINARY-NOISE SOURCE	95
APPENDIX III	
AN ELECTRONIC SPDT SWITCH	98
APPENDIX IV	
A PROGRAM FOR IMPLEMENTING MONTE CARLO METHODS	100
APPENDIX V	
AVERAGE DURATION OF RANDOM WALKS	101
REFERENCES	105

LIST OF ILLUSTRATIONS

	Page
2-1. Space Region Illustrating Defined Terms	7
3-1. Random Walks and Initial and Boundary Conditions of a Typical Problem with 1 Space Variable	32
4-1. Block Diagram for Simulation of a Stochastic Differential Equation	53
4-2. Block Diagram for Generation of γ	54
4-3. Triggering of Mode-Control Flip-Flop	58
4-4. Detection of Termination Time $t = 0$	59
4-5. Boundary Detection for Problems with One Space Variable	60
4-6. Two-Dimensional Region	61
4-7. Two-Dimensional Boundary Detection	62
4-8. Coordinate Transformation used for Boundary Detection of Two-Dimensional Simple Regions	63
4-9. Photograph Illustrating a Detected Boundary	66
4-10. Hybrid Computer System	70
4-11. Flow Diagram for a Typical Hybrid Computer Program.	72
5-1. Solutions of $D_1 \frac{d^2\phi}{dx^2} + K \frac{d\phi}{dx_0} = 0$	74
5-2. Values of $100 \phi_N(0)$ obtained with $N = 1000$	75
5-3. Average Time for a Random Walk used for the Solution of a One-Dimensional Laplace Equation	76
5-4. Solutions of $\frac{d^2\phi}{dx_0^2} - (1 - x_0^2) \phi = 0$	78
5-5. Solutions of Laplace's Equation as a Function of a Boundary Position	80
5-6. Solutions of Poisson's Equation and Laplace's Equation in the Region Shown	82
5-7. Solutions of the Heat Equation used in the Solution of Poisson's Equation	83

	Page
5-8. Solutions of the Heat Equation at the Centre of a Line, a Square and a Cubic Region	85
5-9. Solutions of Laplace's Equation in Three Dimensions	87
AI-1. Interface for Transfer of Data Between PACE and ALWAC	92
AI-2. Instructions for Activating Stepping Motor	94
AII-1. Block Diagram of 3-Channel Noise Source	96
AIII-1. Circuit and Patching for a SPDT Switch	99

ACKNOWLEDGEMENT

Acknowledgement is due to all who have helped during the course of this work. In particular, I would like to express my thanks to Dr. A. C. Soudack, supervisor of this project, for his assistance and encouragement; Dr. F. Noakes, Head of the Electrical Engineering Department, U.B.C., for his interest and support; Mr. H. Kohne for his assistance with the computer hybridization; and Mr. R. E. Butler for many helpful discussions.

Special thanks are given to my wife, Laurie, for her encouragement and help.

Acknowledgement is gratefully given to the National Research Council for Studentships awarded in 1962, 1963, and 1964, and for equipment made available through Block Grants to the Electrical Engineering Department, U.B.C.

1. INTRODUCTION

1.1 Introduction

High-speed computing devices together with sophisticated numerical methods are inadequate for solving many partial differential equations encountered in the study of continuous systems.¹ Numerical methods called Monte Carlo methods are known for solving many functional equations including a class of partial differential equations,² but when implemented on a digital computer the methods have generally proven to be very inefficient.³ In 1960 a Michigan report⁴ outlined a Monte Carlo method using an analog computer for solving a class of homogeneous elliptic partial differential equations. In the Michigan study, solutions were obtained with a slow analog computer at approximately the same rate as that possible with a fast digital computer.

In this project, a hybrid computer is used to implement new Monte Carlo methods that are developed for solving a large class of both elliptic and parabolic partial differential equations. Computing techniques are developed so that, unlike the Michigan study, no special purpose equipment is required. With the hybrid approach, many features, including the capacity to program an entire problem solving procedure and the capacity to obtain automatic printout of all solutions, are made possible.

Most computer methods for solving partial differential equations depend upon approximating the equations by a set of finite-difference equations.^{1,5} The number of difference equations in the set depends geometrically upon the number of

independent variables in the partial differential equation being approximated and upon the precision required in the solution. For many problems the number of difference equations that are required is such that storage and solution times in the case of digital computation, or equipment requirements for analog computation, are entirely unrealistic. Other analog methods⁶ such as solving the set of difference equations with passive lumped elements, electrolytic-tank simulations and membrane analogies are suitable for some problems, but inadequate for many others.

Monte Carlo methods are methods which involve the sampling of random processes* as a means of approximating the solutions of mathematical problems. The random process is related to the problem for which a solution is desired in such a manner that repeated values determined by the process converge in a statistical sense to the solution. For many mathematical problems such a random process cannot be found, and for others, many are known. In the case of partial differential equations, stochastic processes** in the form of random walks can be used to solve equations that are in some way related to diffusion

* A random process is a process exhibiting variations from observation to observation which no amount of effort or control in the course of a run or trial can remove.⁷

** The term stochastic process is used to denote a random process of a time-dependent nature.⁷

processes. Such partial differential equations include two of the three linear second-order canonic types; namely, elliptic (e.g. Laplace's equation) and parabolic (e.g. the diffusion equation) equations. Partial differential equations of the hyperbolic type (e.g. the wave equation) are not amenable to solution by the methods to be discussed.

In all partial differential equations to be considered, the following procedure is used to obtain approximate solutions. A large number of random walks are started in sequence at a point for which a solution is desired, and each random walk is terminated either at a predetermined time or when a boundary is reached. A prescribed value, normally an initial or boundary value, is selected according to the terminal position of each walk, and the average of a large number of such values is determined. As will be shown, this average converges in a statistical sense to the solution at the point where the random walks were started. By this procedure, the solution at all points of interest can be obtained.

In this work, the random walks are generated on the analog computer as the response to random-noise sources. Electronic comparators and function generators on the analog computer are used to determine the terminal positions of the walks. The adjoining digital computer is used to control the analog computer and to average the values associated with the terminal positions of the random walks. This approach takes advantage of the speed with which random walks can be generated on an analog computer as well as the dynamic range and memory capabilities of a digital

computer.

1.2 Thesis Outline

Following this introductory chapter, partial differential equations are derived for certain conditional probability density functions of a class of Markov processes. In Chapter 3, these probability density functions are used to derive Monte Carlo methods that are proposed for solving a large class of homogeneous and nonhomogeneous elliptic, and homogeneous parabolic partial differential equations. The convergence of the Monte Carlo solutions to the exact solution is also considered.

The use of a hybrid computer for solving partial differential equations by Monte Carlo methods is discussed in Chapter 4. Computing techniques, as well as limitations imposed by the equipment, are outlined. Novel methods for detecting boundaries for problems with one, two and three spatial dimensions are also proposed.

Experimental results are given in Chapter 5. The examples in this chapter include solutions of Laplace's equation and Poisson's equation in two and three dimensions, as well as solutions of the heat equation in one, two and three dimensions.

Five appendices follow the conclusions given in Chapter 6. Included in these appendices are the details of the interface that was built to link the two computers⁸ and the description of a new type of multichannel noise source that was developed for this project.⁹

2. FUNDAMENTAL RELATIONS FOR MARKOV PROCESSES

2.1 Introduction

In this chapter certain conditional probability density functions of stochastic processes known as continuous Markov processes are defined and shown to be fundamental solutions of a class of parabolic partial differential equations. The form of the partial differential equations that are developed is closely related to the form of the equations for the boundary-value problems that can be solved by the proposed Monte Carlo methods. In order that the methods apply to partial differential equations of a very general form, a very general Markov process that can be readily simulated on an analog computer is considered.

2.2 Chapman-Kolmogorov Equations for Continuous Markov Processes within Bounded Regions

To solve a boundary-value problem that is defined on an open bounded region R and its boundary C , a continuous Markov process $\bar{r}(t)$, defined on R and C , is considered. In this work, R is assumed to be a one, two or three-dimensional region, and the vector $\bar{r}(t)$ is assumed to have components x , y and z in a cartesian coordinate system.

A continuous Markov process can be defined as a stochastic process having the property that future values of \bar{r} depend upon a time-ordered set of known values of \bar{r} only through the last available value.⁷

That is, if \bar{r} is known to equal \bar{r}_0 at time t_0 , then the value of \bar{r} at some future time t_2 is in no way dependent upon known values of \bar{r} at some earlier time $t_{-1} < t_0$. From this definition it can be shown⁷ that the conditional probability density function $f(\bar{r}_2, t_2 | \bar{r}_0, t_0)$ completely describes the statistical properties of \bar{r} where f is defined as follows.

Definition

$f(\bar{r}_2, t_2 | \bar{r}_0, t_0) dr_2$ is the probability that the random vector \bar{r} is in dr_2 at time t_2 if at time t_0 , $\bar{r} = \bar{r}_0$.

The terms given in the definition are illustrated in Figure 2-1. The differential dr_2 that is used in the definition is an element of generalized volume at the point defined by \bar{r}_2 . That is, dr_2 is either dx_2 , $dx_2 dy_2$ or $dx_2 dy_2 dz_2$ depending upon the dimension of R .

An elementary property of the conditional density function f for a Markov process is that it satisfies the following Chapman-Kolmogorov integral equation⁷

$$f(\bar{r}_2, t_2 | \bar{r}_0, t_0) = \int_R f(\bar{r}_2, t_2 | \bar{r}_1, t_1) f(\bar{r}_1, t_1 | \bar{r}_0, t_0) dr_1 \quad (2.1)$$

for all $t_0 \leq t_1 \leq t_2$.

This equation expresses the fact that a transition of \bar{r} from \bar{r}_0

at t_0 to \bar{r}_2 at t_2 occurs via some point \bar{r}_1 at time t_1 .

In addition to the conditional probability density function f , the following conditional probability density function g , is also defined.

Definition

$g(\bar{r}_b, t_b | \bar{r}_0, t_0) dr_b dt_b$ is the probability that the random vector \bar{r} will reach boundary C within dr_b between times t_b and $t_b + dt_b$ if at time t_0 , $\bar{r} = \bar{r}_0$.

The term dr_b in the definition is a differential element of generalized surface area about a point \bar{r}_b on C . (see Figure 2-1)

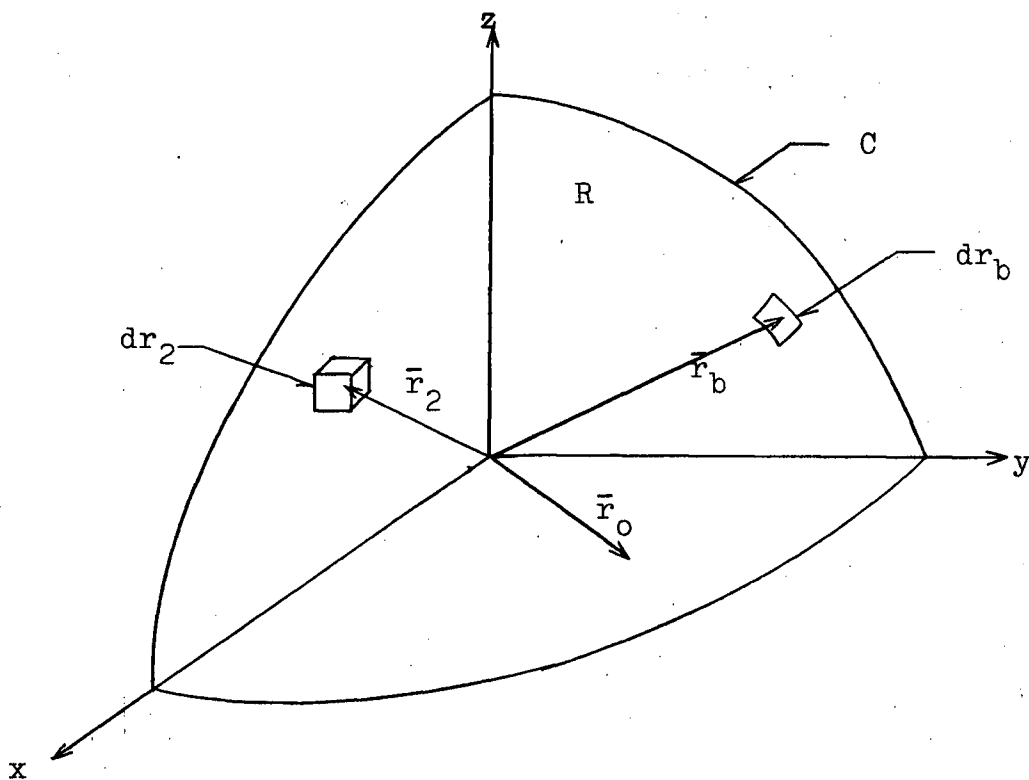


Figure 2-1. Space Region Illustrating Defined Terms

From the Markov property and the fact that a random walk from an interior point \bar{r}_0 at t_0 to a boundary point \bar{r}_b at t_b must pass through some \bar{r}_1 at time $t_1 \leq t_b$, it follows that g must also satisfy a Chapman-Kolmogorov equation; i.e.,

$$g(\bar{r}_b, t_b | \bar{r}_0, t_0) = \int_R g(\bar{r}_b, t_b | \bar{r}_1, t_1) f(\bar{r}_1, t_1 | \bar{r}_0, t_0) d\bar{r}_1 \quad (2.2)$$

for all $t_0 \leq t_1 \leq t_b$.

The Markov processes used for solving partial differential equations are initiated at time t_0 at a point \bar{r}_0 within R , and are terminated either at a predetermined time $t_2 \geq t_0$ or whenever the random variable \bar{r} reaches a boundary point \bar{r}_b on C . Hence, if a process is terminated due to a boundary absorption, it occurs at a time $t_b \leq t_2$. In view of these statements, f and g must satisfy the following initial and boundary conditions.

A. Initial condition for f .

$$\lim_{t_0 \rightarrow t_2} f(\bar{r}_2, t_2 | \bar{r}_0, t_0) = \delta(\bar{r}_2 - \bar{r}_0) \quad (2.3)$$

where

$$\delta(\bar{r}_2 - \bar{r}_0) = 0 \quad \text{for } \bar{r}_2 \neq \bar{r}_0 \quad \text{and} \quad \int_R \delta(\bar{r}_2 - \bar{r}_0) d\bar{r}_2 = 1.$$

This condition expresses the fact that the point of termination \bar{r}_2 is the same as the starting point \bar{r}_0 if the process is terminated immediately after it is initiated.

B. Initial condition for g.

$$\lim_{t_0 \rightarrow t_2} g(\bar{r}_b, t_b | \bar{r}_0, t_0) = 0 \quad (2.4)$$

That is, the probability of reaching a boundary point \bar{r}_b is zero for a walk starting at an interior point \bar{r}_0 when the walk is terminated immediately after it is initiated.

C. Boundary condition for f.

$$\lim_{\bar{r}_0 \rightarrow \bar{r}_b} f(\bar{r}_2, t_2 | \bar{r}_0, t_0) = 0 \quad (2.5)$$

This condition states that if the starting point \bar{r}_0 approaches a boundary point \bar{r}_b there is zero probability that \bar{r} will be in an interior region dr_2 at a time $t_2 \geq t_0$. This is true since the process will terminate immediately at the boundary point \bar{r}_b .

D. Boundary condition for g.

$$\lim_{\bar{r}_0 \rightarrow \bar{r}_b} g(\bar{r}_b, t_b | \bar{r}_0, t_0) = \delta(\bar{r}_0 - \bar{r}_b) \delta(t_b - t_0) \quad (2.6)$$

where

$$\delta(\bar{r}_0 - \bar{r}_b) \delta(t_b - t_0) = 0 \quad \text{unless} \quad \bar{r}_0 = \bar{r}_b \quad \text{and} \quad t_b = t_0$$

$$\text{and } \int_{t_0}^{t_2} \int_C \delta(\bar{r}_0 - \bar{r}_b) \delta(t_b - t_0) dr_b dt_b = 1$$

As the interior starting point \bar{r}_0 approaches a boundary point \bar{r}_b , the process is certain to terminate immediately at the point \bar{r}_b .

In addition to these initial and boundary conditions, the following integral relation must also be valid for all \bar{r}_0 and t_0 :

$$\int_R f(\bar{r}_2, t_2 | \bar{r}_0, t_0) dr_2 + \int_{t_0}^{t_2} \int_C g(\bar{r}_b, t_b | \bar{r}_0, t_0) dr_b dt_b = 1 \quad (2.7)$$

The first term of this equation is the probability that \bar{r} is within the boundary at time t_2 , and the second term is the probability that \bar{r} has reached a boundary within time t_2 . Since one of the two events must be true, the sum of the two terms is unity.

In the following section the Chapman-Kolmogorov integral equations (2.1) and (2.2) are converted to second-order partial differential equations.

2.3 Backward Kolmogorov Partial Differential Equations

The Chapman-Kolmogorov integral equations of the previous section are converted to partial differential equations by expanding a term in the integrands of the integral equations

in a Taylor series about the initial point \bar{r}_0 , and then taking a limit. For a general Markov process all terms of the Taylor series are required in the expansions, but for Markov processes in which the random variable \bar{r} changes by only a small amount in a small time interval Δt , only the first two terms of the series contribute when the limit is taken. The resulting second-order partial differential equations are called backward Kolmogorov equations.¹⁰

Consider Chapman-Kolmogorov equation (2.1) for $t_1 = t_0 + \Delta t$; i.e.,

$$f(\bar{r}_2, t_2 | \bar{r}_0, t_0) = \int_R f(\bar{r}_2, t_2 | \bar{r}_1, t_0 + \Delta t) f(\bar{r}_1, t_0 + \Delta t | \bar{r}_0, t_0) dr_1 \quad (2.8)$$

For Δt small, the term $f(\bar{r}_1, t_0 + \Delta t | \bar{r}_0, t_0)$ is the incremental transition probability density of the process. It gives the distribution of displacements after a small time Δt . If after Δt the displacement from \bar{r}_0 is so small that the probability of reaching a boundary is zero, it follows from equation (2.7) that

$$\lim_{\Delta t \rightarrow 0} \int_R f(\bar{r}_1, t_0 + \Delta t | \bar{r}_0, t_0) dr_1 = 1 \quad (2.9)$$

To convert equation (2.8) into a partial differential equation, the term $f(\bar{r}_2, t_2 | \bar{r}_1, t_0 + \Delta t)$ in the equation is

expanded in a Taylor series about \bar{r}_0 . For the expansion, all variables but \bar{r}_1 are assumed to be fixed. The expansion yields

$$\begin{aligned}
 f(\bar{r}_2, t_2 | \bar{r}_0, t_0) &= \int_R \left[f(\bar{r}_2, t_2 | \bar{r}_0, t_0 + \Delta t) \right. \\
 &+ \frac{\partial f(\bar{r}_2, t_2 | \bar{r}_0, t_0 + \Delta t)}{\partial x_0} (x_1 - x_0) \\
 &+ \frac{\partial f(\bar{r}_2, t_2 | \bar{r}_0, t_0 + \Delta t)}{\partial y_0} (y_1 - y_0) \\
 &+ \frac{\partial f(\bar{r}_2, t_2 | \bar{r}_0, t_0 + \Delta t)}{\partial z_0} (z_1 - z_0) \\
 &+ \frac{\partial^2 f(\bar{r}_2, t_2 | \bar{r}_0, t_0 + \Delta t)}{\partial x_0 \partial y_0} (x_1 - x_0)(y_1 - y_0) \\
 &+ \frac{\partial^2 f(\bar{r}_2, t_2 | \bar{r}_0, t_0 + \Delta t)}{\partial x_0 \partial z_0} (x_1 - x_0)(z_1 - z_0) \\
 &+ \frac{\partial^2 f(\bar{r}_2, t_2 | \bar{r}_0, t_0 + \Delta t)}{\partial y_0 \partial z_0} (y_1 - y_0)(z_1 - z_0) \\
 &+ \frac{1}{2} \frac{\partial^2 f(\bar{r}_2, t_2 | \bar{r}_0, t_0 + \Delta t)}{\partial x_0^2} (x_1 - x_0)^2 \\
 &+ \frac{1}{2} \frac{\partial^2 f(\bar{r}_2, t_2 | \bar{r}_0, t_0 + \Delta t)}{\partial y_0^2} (y_1 - y_0)^2 \\
 &+ \frac{1}{2} \frac{\partial^2 f(\bar{r}_2, t_2 | \bar{r}_0, t_0 + \Delta t)}{\partial z_0^2} (z_1 - z_0)^2
 \end{aligned}$$

$$+ \text{higher-order terms} \left] f(\bar{r}_1, t_0 + \Delta t | \bar{r}_0, t_0) dr_1 \quad (2.10)$$

- If,
1. terms not involving x_1 , y_1 or z_1 are taken outside the integral,
 2. equation (2.9) is used,
 3. all terms are divided by Δt , and the following limits are assumed;

$$\lim_{\Delta t \rightarrow 0} \frac{1}{\Delta t} \int_R (x_1 - x_0) f(\bar{r}_1, t_0 + \Delta t | \bar{r}_0, t_0) dr_1 = a_1(\bar{r}_0, t_0) \quad (2.11)$$

$$\lim_{\Delta t \rightarrow 0} \frac{1}{\Delta t} \int_R (y_1 - y_0) f(\bar{r}_1, t_0 + \Delta t | \bar{r}_0, t_0) dr_1 = a_2(\bar{r}_0, t_0) \quad (2.12)$$

$$\lim_{\Delta t \rightarrow 0} \frac{1}{\Delta t} \int_R (z_1 - z_0) f(\bar{r}_1, t_0 + \Delta t | \bar{r}_0, t_0) dr_1 = a_3(\bar{r}_0, t_0) \quad (2.13)$$

$$\lim_{\Delta t \rightarrow 0} \frac{1}{2\Delta t} \int_R (x_1 - x_0)^2 f(\bar{r}_1, t_0 + \Delta t | \bar{r}_0, t_0) dr_1 = b_1(\bar{r}_0, t_0) \quad (2.14)$$

$$\lim_{\Delta t \rightarrow 0} \frac{1}{2\Delta t} \int_R (y_1 - y_0)^2 f(\bar{r}_1, t_0 + \Delta t | \bar{r}_0, t_0) dr_1 = b_2(\bar{r}_0, t_0) \quad (2.15)$$

$$\lim_{\Delta t \rightarrow 0} \frac{1}{2\Delta t} \int_R (z_1 - z_0)^2 f(\bar{r}_1, t_0 + \Delta t | \bar{r}_0, t_0) dr_1 = b_3(\bar{r}_0, t_0) \quad (2.16)$$

$$\lim_{\Delta t \rightarrow 0} \frac{1}{\Delta t} \int_R (x_1 - x_0)(y_1 - y_0) f(\bar{r}_1, t_0 + \Delta t | \bar{r}_0, t_0) dr_1 = c_1(\bar{r}_0, t_0) \quad (2.17)$$

$$\lim_{\Delta t \rightarrow 0} \frac{1}{\Delta t} \int_R (x_1 - x_0)(z_1 - z_0) f(\bar{r}_1, t_0 + \Delta t | \bar{r}_0, t_0) dr_1 = c_2(\bar{r}_0, t_0) \quad (2.18)$$

$$\lim_{\Delta t \rightarrow 0} \frac{1}{\Delta t} \int_R (y_1 - y_0)(z_1 - z_0) f(\bar{r}_1, t_0 + \Delta t | \bar{r}_0, t_0) dr_1 = c_3(\bar{r}_0, t_0) \quad (2.19)$$

$$\lim_{\Delta t \rightarrow 0} \frac{1}{\Delta t} \int_R (\text{higher-order terms}) f(\bar{r}_1, t_0 + \Delta t | \bar{r}_0, t_0) dr_1 = 0 \quad (2.20)$$

$$\lim_{\Delta t \rightarrow 0} \frac{f(\bar{r}_2, t_2 | \bar{r}_0, t_0 + \Delta t) - f(\bar{r}_2, t_2 | \bar{r}_0, t_0)}{\Delta t} = \frac{\partial f}{\partial t_0}(\bar{r}_2, t_2 | \bar{r}_0, t_0) \quad (2.21)$$

then equation (2.10) becomes

$$\begin{aligned} - \frac{\partial f}{\partial t_0}(\bar{r}_2, t_2 | \bar{r}_0, t_0) &= a_1(\bar{r}_0, t_0) \frac{\partial f}{\partial x_0} + a_2(\bar{r}_0, t_0) \frac{\partial f}{\partial y_0} + a_3(\bar{r}_0, t_0) \frac{\partial f}{\partial z_0} \\ &+ b_1(\bar{r}_0, t_0) \frac{\partial^2 f}{\partial x_0^2} + b_2(\bar{r}_0, t_0) \frac{\partial^2 f}{\partial y_0^2} + b_3(\bar{r}_0, t_0) \frac{\partial^2 f}{\partial z_0^2} \\ &+ c_1(\bar{r}_0, t_0) \frac{\partial^2 f}{\partial x_0 \partial y_0} + c_2(\bar{r}_0, t_0) \frac{\partial^2 f}{\partial x_0 \partial z_0} + c_3(\bar{r}_0, t_0) \frac{\partial^2 f}{\partial y_0 \partial z_0} \end{aligned} \quad (2.22)$$

This equation is known as a backward Kolmogorov equation. In Section 2.4 a particular Markov process for which the backward Kolmogorov equation is valid will be considered.

Backward Kolmogorov equation (2.22) can be written conveniently in terms of an operator $L_{\bar{r}_0, t_0}$ as

$$-\frac{\partial f(\bar{r}_2, t_2 | \bar{r}_0, t_0)}{\partial t_0} = L_{\bar{r}_0, t_0} f(\bar{r}_2, t_2 | \bar{r}_0, t_0) \quad (2.23)$$

where

$$\begin{aligned} L_{\bar{r}_0, t_0} &= a_1(\bar{r}_0, t_0) \frac{\partial}{\partial x_0} + a_2(\bar{r}_0, t_0) \frac{\partial}{\partial y_0} + a_3(\bar{r}_0, t_0) \frac{\partial}{\partial z_0} \\ &+ b_1(\bar{r}_0, t_0) \frac{\partial^2}{\partial x_0^2} + b_2(\bar{r}_0, t_0) \frac{\partial^2}{\partial y_0^2} + b_3(\bar{r}_0, t_0) \frac{\partial^2}{\partial z_0^2} \\ &+ c_1(\bar{r}_0, t_0) \frac{\partial^2}{\partial x_0 \partial y_0} + c_2(\bar{r}_0, t_0) \frac{\partial^2}{\partial x_0 \partial z_0} \\ &+ c_3(\bar{r}_0, t_0) \frac{\partial^2}{\partial y_0 \partial z_0} \end{aligned} \quad (2.24)$$

The subscripts \bar{r}_0 and t_0 are used to indicate that the operator is a function of \bar{r}_0 and t_0 and that differential operations are with respect to components x_0, y_0 and z_0 of the initial position vector \bar{r}_0 . The vector \bar{r}_2 and time t_2 are parameters in the partial differential equation. To clarify the notation, equation (2.23) in one dimension is

$$\begin{aligned}
-\frac{\partial f(x_2, t_2 | x_0, t_0)}{\partial t_0} &= a_1(x_0, t_0) \frac{\partial f(x_2, t_2 | x_0, t_0)}{\partial x_0} \\
&+ b_1(x_0, t_0) \frac{\partial^2 f(x_2, t_2 | x_0, t_0)}{\partial x_0^2}
\end{aligned} \tag{2.25}$$

By a procedure similar to that carried out above, the Chapman-Kolmogorov equation (2.2) for $g(\bar{r}_b, t_b | \bar{r}_0, t_0)$ can be converted to a backward Kolmogorov equation. In this case $g(\bar{r}_b, t_b | \bar{r}_1, t_0 + \Delta t)$ is expanded in a Taylor series about \bar{r}_0 . Using the previously defined limits (2.11) to (2.21) and the operator notation, it follows that

$$-\frac{\partial g(\bar{r}_b, t_b | \bar{r}_0, t_0)}{\partial t_0} = L_{\bar{r}_0, t_0} g(\bar{r}_b, t_b | \bar{r}_0, t_0) \tag{2.26}$$

The partial differential equations that have been derived will be used in Chapter 3 to derive Monte Carlo methods for solving boundary-value problems that are governed by equations of a form similar to (2.26). However, before proceeding to Chapter 3, a Markov process that gives rise to limits (2.11) to (2.21) and a method for generalizing the Kolmogorov equations will be considered.

2.4 A Continuous Markov Process for which Backward Kolmogorov Equations are Valid

In the Monte Carlo methods to be outlined, the coefficients in the Kolmogorov equations coincide with the coefficients in the partial differential equations for which the methods are applicable. It is therefore necessary to consider a Markov process for which the assumed limits (2.11) to (2.21) are valid. A mathematical model of such a process is defined by the following set of stochastic differential equations:

$$\frac{dx}{dt} + A_1(x, y, z, t) = B_1(x, y, z, t)N_1(t) \quad (2.27)$$

$$\frac{dy}{dt} + A_2(x, y, z, t) = B_2(x, y, z, t)N_2(t) \quad (2.28)$$

$$\frac{dz}{dt} + A_3(x, y, z, t) = B_3(x, y, z, t)N_3(t) \quad (2.29)$$

These equations can be written in matrix form as

$$\frac{d\bar{r}}{dt} + A(\bar{r}, t) = B(\bar{r}, t)N(t) \quad (2.30)$$

The dependent variables x , y and z in this model are the components of the random vector \bar{r} , for which density functions f and g have been defined. The coefficients A_i and B_i are, in general, slowly varying continuous functions of x , y , z and t . The driving terms $N_i(t)$ are uncorrelated with each other, and each term is stationary Gaussian white noise with

zero average. These properties of $N_i(t)$ are expressed in the following manner:

$$\langle N_i(t) \rangle = 0 \quad (2.31)$$

$$\langle N_i(t_1)N_i(t_2) \rangle = 2D_i \delta(t_1 - t_2) \quad (2.32)$$

$$\langle N_i(t)N_j(t) \rangle = 0 \quad (2.33)$$

$$\langle N_i(t_1)N_i(t_2) \dots N_i(t_{2m+1}) \rangle = 0 \quad (2.34)$$

$$\begin{aligned} & \langle N_i(t_1)N_i(t_2) \dots N_i(t_{2m}) \rangle \quad (2.35) \\ & = \sum_{\text{all pairs}} \langle N_i(t_i)N_i(t_j) \rangle \langle N_i(t_k)N_i(t_l) \rangle \dots \end{aligned}$$

In these equations the brackets $\langle \rangle$ signify an ensemble average. $\delta(t)$ is the unit impulse function, and $2D_i$ is the power spectral density of $N_i(t)$. Equations (2.34) and (2.35), or similar equations, are required in order to show that the limits of the higher-order moments (2.20) are actually zero. The properties that have been assumed for the model imply that each $N_i(t)$ has a Gaussian distributed amplitude.¹¹ In equation (2.35), the sum is to be taken over the $\frac{(2m)!}{2^m m!}$ possible ways that $2m$ points can be divided into m pairs.

To show that the process defined by equation (2.30)

is actually a Markov process, it is sufficient to show that, given $\bar{r}(t_0) = \bar{r}_0$, the statistics of $\bar{r}(t_1)$ are in no way affected by the additional information that $\bar{r}(t_{-1}) = \bar{r}_{-1}$ where $t_{-1} < t_0 < t_1$. From equation (2.30),

$$\bar{r}(t_1) = \bar{r}_0 + \int_{t_0}^{t_1} [B(\bar{r}, t)N(t) - A(\bar{r}, t)] dt \quad (2.36)$$

Since $\bar{r}(t_0) = \bar{r}_0$ is fixed, the statistics of $\bar{r}(t_1)$ depend only upon the statistics of the driving vector $N(t)$ in the interval (t_0, t_1) . If the additional information $\bar{r}(t_{-1}) = \bar{r}_{-1}$ is also given, then

$$\int_{t_{-1}}^{t_0} [B(\bar{r}, t)N(t) - A(\bar{r}, t)] dt = \bar{r}_0 - \bar{r}_{-1} \quad (2.37)$$

This condition on the integral provides information about $N(t)$ in the interval (t_{-1}, t_0) , but does not give any information about $N(t)$ in (t_0, t_1) , since by equation (2.32), $N(t)$ in the two intervals is uncorrelated. The statistics of $\bar{r}(t_1)$ therefore do not depend upon the additional information $\bar{r}(t_{-1}) = \bar{r}_{-1}$. Hence, $\bar{r}(t)$ is indeed a Markov process.

The limits (2.11) to (2.20) of the Markov process given by equations (2.27) to (2.29) are calculated by integrating the equations between $t = t_0$ and $t = t_0 + \Delta t$ and then

taking the required ensemble averages and limits. Consider equation (2.27) with the coefficients written in vector notation.

Integration gives

$$(\mathbf{x}_1 - \mathbf{x}_0) = - \int_{t_0}^{t_0 + \Delta t} A_1(\bar{\mathbf{r}}, t) dt + \int_{t_0}^{t_0 + \Delta t} B_1(\bar{\mathbf{r}}, t) N_1(t) dt \quad (2.38)$$

Under the condition that $A_1(\bar{\mathbf{r}}, t)$ and $B_1(\bar{\mathbf{r}}, t)$ vary at a much slower rate than $N_1(t)$, this equation can be written

$$(\mathbf{x}_1 - \mathbf{x}_0) = - A_1(\bar{\mathbf{r}}_0, t_0) \Delta t + B_1(\bar{\mathbf{r}}_0, t_0) \int_{t_0}^{t_0 + \Delta t} N_1(t) dt + o(\Delta t) \quad (2.39)$$

where $\lim_{\Delta t \rightarrow 0} \frac{o(\Delta t)}{\Delta t} = 0$ (2.40)

The ensemble average of the n^{th} power of $(\mathbf{x}_1 - \mathbf{x}_0)$ is expressed by the Binomial Theorem as

$$\begin{aligned} \langle (\mathbf{x}_1 - \mathbf{x}_0)^n \rangle &= \sum_{k=0}^n \frac{n!}{k!(n-k)!} \left[-A_1(\bar{\mathbf{r}}_0, t_0) \Delta t \right]^{n-k} \left[B_1(\bar{\mathbf{r}}_0, t_0) \right]^k \\ &\int_{t_0}^{t_0 + \Delta t} \cdots \int_{t_0}^{t_0 + \Delta t} \langle N_1(t_1) N_1(t_2) \cdots N_1(t_k) \rangle dt_1 dt_2 \cdots dt_k + o(\Delta t) \end{aligned} \quad (2.41)$$

where, for $k = 0$, the multiple integral is unity.

From conditions (2.32), (2.34) and (2.35),

$$\int_{t_0}^{t_0 + \Delta t} \dots \int \left\langle N_1(t_1) N_1(t_2) \dots N_1(t_k) \right\rangle dt_1 dt_2 \dots dt_k = 0$$

for k odd (2.42)

$$= \frac{k!}{2^{\frac{k}{2}} (\frac{k}{2})!} (2D_1)^{\frac{k}{2}} (\Delta t)^{\frac{k}{2}}$$

for k even (2.43)

Hence,

$$\left\langle (x_1 - x_0)^n \right\rangle = -A_1(\bar{r}_0, t_0) \Delta t + o(\Delta t) \quad \text{for } n = 1 \quad (2.44)$$

$$= 2 \left[B_1(\bar{r}_0, t_0) \right]^2 D_1 \Delta t + o(\Delta t)$$

for $n = 2$ (2.45)

$$= o(\Delta t) \quad \text{for } n \geq 3 \quad (2.46)$$

The limits $a_1(\bar{r}_0, t_0)$, $b_1(\bar{r}_0, t_0)$ and a higher-order limit are obtained directly from these expressions by dividing by Δt and taking the limit. By a similar procedure, it follows that all the limiting conditions that were assumed in Section 2.3 are valid for the Markov process defined by equations (2.27) to (2.29). For completeness, all relationships between the limits, or coefficients in the Kolmogorov equations, and the coefficients in the stochastic differential equations (2.27) to (2.29) are

listed below:

$$a_1(\bar{r}_0, t_0) = -A_1(\bar{r}_0, t_0) \quad (2.47)$$

$$a_2(\bar{r}_0, t_0) = -A_2(\bar{r}_0, t_0) \quad (2.48)$$

$$a_3(\bar{r}_0, t_0) = -A_3(\bar{r}_0, t_0) \quad (2.49)$$

$$b_1(\bar{r}_0, t_0) = \left[B_1(\bar{r}_0, t_0) \right]^2 D_1 \quad (2.50)$$

$$b_2(\bar{r}_0, t_0) = \left[B_2(\bar{r}_0, t_0) \right]^2 D_2 \quad (2.51)$$

$$b_3(\bar{r}_0, t_0) = \left[B_3(\bar{r}_0, t_0) \right]^2 D_3 \quad (2.52)$$

$$c_1(\bar{r}_0, t_0) = c_2(\bar{r}_0, t_0) = c_3(\bar{r}_0, t_0) = 0 \quad (2.53)$$

The fact that coefficients $c_i(\bar{r}_0, t_0)$ are zero is a consequence of the assumption that the noise terms $N_i(t)$ are not correlated with each other. This assumption is not necessary in theory, but in practice it would be extremely difficult to realize noise sources with specified crosscorrelation as well as autocorrelation.

A Markov process giving rise to conditional probability density functions f and g that satisfy Kolmogorov partial differential equations (2.23) and (2.26) has been discussed. In the following section, auxiliary probability density functions that satisfy more general partial differential equations than the Kolmogorov equations will be studied.

2.5 Partial Differential Equations Satisfied by Auxiliary Probability Density Functions

The second-order Kolmogorov equations that have been derived are the basis of Monte Carlo methods for solving partial differential equations. The Kolmogorov equations, however, only contain terms in the derivatives of the density functions f and g , which means that only problems yielding partial differential equations of this form can be treated. An extended form of the Kolmogorov equations containing the dependent variable itself can be obtained by considering auxiliary density functions¹² u and v defined below. These auxiliary functions are obtained from the same Markov process as considered in the previous section by weighting the probability density functions f and g . With this extension, partial differential equations containing a term in the dependent variable itself can be solved.

The auxiliary probability density functions u and v are defined as follows:

$$u(\bar{r}_2, t_2 | \bar{r}_0, t_0) = \left\langle \exp -m(t_2, t_0) \right\rangle_{\substack{\bar{r}(t_2) = \bar{r}_2 \\ \bar{r}(t_0) = \bar{r}_0}} f(\bar{r}_2, t_2 | \bar{r}_0, t_0) \quad (2.54)$$

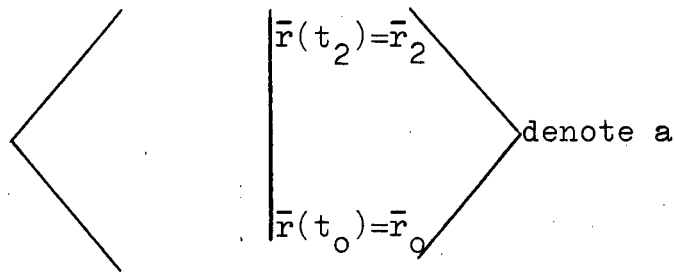
$$v(\bar{r}_b, t_b | \bar{r}_0, t_0) = \left\langle \exp -m(t_b, t_0) \right\rangle_{\substack{\bar{r}(t_b) = \bar{r}_b \\ \bar{r}(t_0) = \bar{r}_0}} g(\bar{r}_b, t_b | \bar{r}_0, t_0) \quad (2.55)$$

The term $m(t_2, t_0)$ is given by the functional

$$m(t_2, t_0) = \int_{t_0}^{t_2} d[\bar{r}(t), t] dt \quad (2.56)$$

where $d[\bar{r}(t), t]$ is a continuous positive function of the random vector $\bar{r}(t)$ and time t .

The brackets



conditional expectation; that is, the expected value of the function within the brackets subject to the conditions that $\bar{r}(t_0) = \bar{r}_0$ and $\bar{r}(t_2)$ is in a small region dr_2 about \bar{r}_2 .

In a manner similar to that given by Darling and Siegert,¹² it will be shown that $u(\bar{r}_2, t_2 | \bar{r}_0, t_0)$ and $v(\bar{r}_b, t_b | \bar{r}_0, t_0)$ satisfy the following partial differential equations:

$$-\frac{\partial u(\bar{r}_2, t_2 | \bar{r}_0, t_0)}{\partial t_0} = L_{\bar{r}_0, t_0} u(\bar{r}_2, t_2 | \bar{r}_0, t_0) - d(\bar{r}_0, t_0) u(\bar{r}_2, t_2 | \bar{r}_0, t_0) \quad (2.57)$$

$$-\frac{\partial v(\bar{r}_b, t_b | \bar{r}_0, t_0)}{\partial t_0} = L_{\bar{r}_0, t_0} v(\bar{r}_b, t_b | \bar{r}_0, t_0) - d(\bar{r}_0, t_0) v(\bar{r}_b, t_b | \bar{r}_0, t_0) \quad (2.58)$$

From the identity

$$\exp -m(t_2, t_0) = 1 - \int_{t_0}^{t_2} \frac{\partial}{\partial t_1} \exp -m(t_2, t_1) dt_1 \quad (2.59)$$

and the relation

$$\frac{\partial}{\partial t_1} m(t_2, t_1) = -d[\bar{r}(t_1), t_1] \quad (2.60)$$

it follows that

$$\exp -m(t_2, t_0) = 1 - \int_{t_0}^{t_2} d[r(t_1), t_1] \exp -m(t_2, t_1) dt_1 \quad (2.61)$$

Taking the conditional expectation of both sides of this equation, multiplying by $f(\bar{r}_2, t_2 | \bar{r}_0, t_0)$ and applying definition (2.54), gives

$$u(\bar{r}_2, t_2 | \bar{r}_0, t_0) = f(\bar{r}_2, t_2 | \bar{r}_0, t_0) -$$

$$\int_{t_0}^{t_2} \left\langle d[\bar{r}(t_1), t_1] \exp -m(t_2, t_1) \right\rangle dt_1 f(\bar{r}_2, t_2 | \bar{r}_0, t_0) \quad (2.62)$$

The conditional expectation, if $\bar{r}(t_1)$ is considered fixed at \bar{r}_1 , can be written

$$\int_R \left\langle d[\bar{r}(t_1), t_1] \exp -m(t_2, t_1) \right\rangle_{\substack{\bar{r}(t_2) = \bar{r}_2 \\ \bar{r}(t_0) = \bar{r}_0}} = \int_R d(\bar{r}_1, t_1) \exp -m(t_2, t_1) p(\bar{r}_1, t_1 | \bar{r}_0, t_0; \bar{r}_2, t_2) dr_1 \quad (2.63)$$

where $p(\bar{r}_1, t_1 | \bar{r}_0, t_0; \bar{r}_2, t_2) dr_1$ is the probability that the random variable \bar{r} is in the region dr_1 at t_1 if it is given that \bar{r} is at \bar{r}_0 and in the region dr_2 at times t_0 and t_2 respectively. For a Markov process

$$p(\bar{r}_1, t_1 | \bar{r}_0, t_0; \bar{r}_2, t_2) f(\bar{r}_2, t_2 | \bar{r}_0, t_0) = f(\bar{r}_1, t_1 | \bar{r}_0, t_0) f(\bar{r}_2, t_2 | \bar{r}_1, t_1) \quad (2.64)$$

Now, since \bar{r}_1 , within the conditional expectation, is fixed, $d(\bar{r}_1, t_1)$ in the second member of equation (2.63) can be taken outside the conditional expectation. Also, for $\bar{r}(t)$ a Markov process, $\bar{r}(t_2)$ is independent of $\bar{r}(t_0)$ when $\bar{r}(t_1) = \bar{r}_1$ is given and $t_2 > t_1 > t_0$. The condition $\bar{r}(t_0) = \bar{r}_0$ can therefore be deleted from the conditional expectation.

Therefore,

$$\begin{aligned}
 & \left\langle d[\bar{r}(t_1), t_1] \exp -m(t_2, t_1) \right| \begin{array}{l} \bar{r}(t_2) = \bar{r}_2 \\ \bar{r}(t_0) = \bar{r}_0 \end{array} \right\rangle = \\
 & \int_R d(\bar{r}_1, t_1) \left\langle \exp -m(t_2, t_1) \right| \begin{array}{l} \bar{r}(t_2) = \bar{r}_2 \\ \bar{r}(t_1) = \bar{r}_1 \end{array} \right\rangle \cdot \\
 & \frac{f(\bar{r}_1, t_1 | \bar{r}_0, t_0) f(\bar{r}_2, t_2 | \bar{r}_1, t_1) d\bar{r}_1}{f(\bar{r}_2, t_2 | \bar{r}_0, t_0)} \quad (2.65)
 \end{aligned}$$

Substituting equation (2.65) back into equation (2.62), and using the definition of $u(\bar{r}_2, t_2 | \bar{r}_1, t_1)$ gives

$$u(\bar{r}_2, t_2 | \bar{r}_0, t_0) = f(\bar{r}_2, t_2 | \bar{r}_0, t_0) -$$

$$\int_{t_0}^{t_2} \int_R d(\bar{r}_1, t_1) u(\bar{r}_2, t_2 | \bar{r}_1, t_1) f(\bar{r}_1, t_1 | \bar{r}_0, t_0) d\bar{r}_1 dt_1 \quad (2.66)$$

If the order of integration is reversed and both sides of the equation are operated upon with the operator $L_{\bar{r}_0, t_0} + \frac{\partial}{\partial t_0}$, where from (2.23)

$$\left(L_{\bar{r}_0, t_0} + \frac{\partial}{\partial t_0} \right) f(\bar{r}_2, t_2 | \bar{r}_0, t_0) = 0$$

the following equation is obtained:

$$\begin{aligned} & \left(L_{\bar{r}_0, t_0} + \frac{\partial}{\partial t_0} \right) u(\bar{r}_2, t_2 | \bar{r}_0, t_0) = \\ & \int_R d(\bar{r}_1, t_0) u(\bar{r}_2, t_2 | \bar{r}_1, t_0) f(\bar{r}_1, t_0 | \bar{r}_0, t_0) dr_1 \end{aligned} \quad (2.67)$$

From equation (2.3), however,

$$\lim_{t_1 \rightarrow t_0} f(\bar{r}_1, t_1 | \bar{r}_0, t_0) = \delta(\bar{r}_1 - \bar{r}_0)$$

Therefore,

$$- \frac{\partial}{\partial t_0} u(\bar{r}_2, t_2 | \bar{r}_0, t_0) = L_{\bar{r}_0, t_0} u(\bar{r}_2, t_2 | \bar{r}_0, t_0) - d(\bar{r}_0, t_0) u(\bar{r}_2, t_2 | \bar{r}_0, t_0) \quad (2.57)$$

as was to be shown.

By a similar analysis, with $p(\bar{r}_1, t_1 | \bar{r}_0, t_0; \bar{r}_2, t_2)$ replaced by $q(\bar{r}_1, t_1 | \bar{r}_0, t_0; \bar{r}_b, t_b)$, where

$$\begin{aligned} q(\bar{r}_1, t_1 | \bar{r}_0, t_0; \bar{r}_b, t_b) g(\bar{r}_b, t_b | \bar{r}_0, t_0) = \\ f(\bar{r}_1, t_1 | \bar{r}_0, t_0) g(\bar{r}_b, t_b | \bar{r}_1, t_1) \end{aligned} \quad (2.68)$$

it follows that $v(\bar{r}_b, t_b \mid \bar{r}_o, t_o)$ satisfies equation (2.58).

It is important to note that the auxiliary density functions u and v satisfy the same initial and boundary conditions (2.3) to (2.6) as f and g respectively. This follows from definitions (2.54) and (2.55).

The form of the initial and boundary conditions for the partial differential equations developed in this chapter suggests that the density functions f , g , u and v can be regarded as fundamental solutions or Green's functions for boundary-value problems. This property will be studied in the following chapter.

3. MONTE CARLO METHODS FOR THE SOLUTIONS OF BOUNDARY-VALUE PROBLEMS

3.1 Introduction

In this chapter relationships between probability density functions f , g , u and v and solutions ϕ of boundary-value problems will be developed. The methods to be described can be applied to problems governed by partial differential equations of the same form as those for f , g , u and v in which ϕ itself is given initially and on all boundaries.

In all problems to be considered, the solution at a point is obtained as the expected value of initial and boundary values at the terminal points of random walks originating at the point for which the solution is desired. The expected value is written in terms of the probability density functions f and g , or u and v . An approximation to the expected value is determined experimentally from a large number of random walks simulated on an analog computer. The approximation converges in a statistical sense to the true solution as the number of random walks increases.

The form of the partial differential equations in Problems A and B is not standard in that a minus sign precedes the time derivatives. This form is convenient for the analysis, and in no way restricts the methods since the equations of an actual problem can always be transformed to the required form by defining a new time variable.

Methods for solving the various classes of problems will now be outlined.

3.2 Solutions of Boundary-Value Problems for Parabolic Partial Differential Equations

The statement of the problem to be considered in this section is as follows.

Problem A Determine $\phi(\bar{r}_0, t_0)$ such that:

$$(1) \quad - \frac{\partial \phi(\bar{r}_0, t_0)}{\partial t_0} = L_{\bar{r}_0, t_0} \phi(\bar{r}_0, t_0) \quad (3.1)$$

is satisfied within a bounded region R;

(2) a piecewise continuous initial condition $\phi_0(\bar{r}_0)$ is satisfied within R; i.e.,

$$\phi(\bar{r}_0, 0) = \phi_0(\bar{r}_0); \quad (3.2)$$

(3) a piecewise continuous boundary condition

$\phi_c(\bar{r}_b, t_0)$ is satisfied on the boundary

C of R; i.e.,

$$\phi(\bar{r}_b, t_0) = \phi_c(\bar{r}_b, t_0). \quad (3.3)$$

The boundaries and initial and boundary conditions of a typical problem with one space variable are shown in Figure 3-1. The time variable t that is shown in the figure is such that $\phi(\bar{r}_0, t_0)$ is defined for $t_0 \leq 0$.

To determine the solution ϕ of Problem A at a point (\bar{r}_0, t_0) , random walks are started at point (\bar{r}_0, t_0) . Each walk is terminated as soon as a boundary is reached or at $t = 0$. If a walk terminates on a boundary at (\bar{r}_b, t_b) the boundary value $\phi_c(\bar{r}_b, t_b)$ is recorded, whereas if a walk is terminated at $t = 0$ with position \bar{r}_2 , the initial value $\phi_0(\bar{r}_2)$ is recorded. It

will be shown that the expected value of the recorded boundary and initial values is a solution of Problem A.

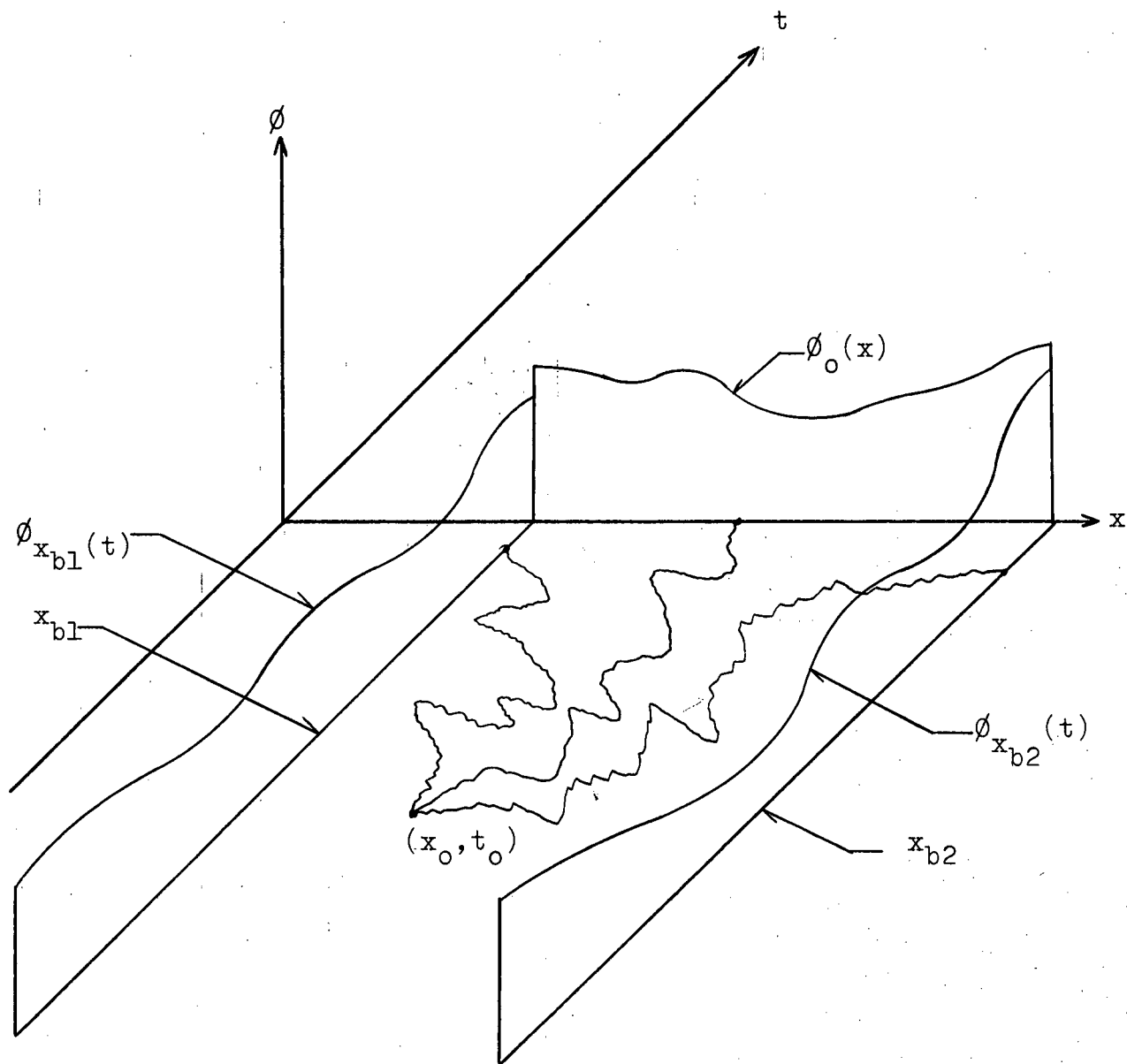


Figure 3-1. Random Walks and Initial and Boundary Conditions of a Typical Problem with 1 Space Variable.

The expected value of the initial and boundary values can be written in terms of the probability density functions $f(\bar{r}_2, 0 \mid \bar{r}_0, t_0)$ and $g(\bar{r}_b, t_b \mid \bar{r}_0, t_0)$ as

$$\begin{aligned} \phi(\bar{r}_0, t_0) = & \int_R \phi_0(\bar{r}_2) f(\bar{r}_2, 0 \mid \bar{r}_0, t_0) dr_2 \\ & + \int_{t_0}^0 \int_C \phi_c(\bar{r}_b, t_b) g(\bar{r}_b, t_b \mid \bar{r}_0, t_0) dr_b dt_b \end{aligned} \quad (3.4)$$

where it has been assumed that the expected value is the solution. It must be proven that $\phi(\bar{r}_0, t_0)$ as given by equation (3.4) is actually a solution of Problem A.

To prove that $\phi(\bar{r}_0, t_0)$ satisfies the partial differential equation of Problem A, operate on equation (3.4) with the operator $\frac{\partial}{\partial t_0} + L_{\bar{r}_0, t_0}$. Since the operator is with respect to \bar{r}_0 and t_0 , the result is

$$\begin{aligned}
\left(\frac{\partial}{\partial t_0} + L_{\bar{r}_0, t_0}\right) \phi(\bar{r}_0, t_0) &= \int_R \phi_0(\bar{r}_2) \left(\frac{\partial}{\partial t_0} + L_{\bar{r}_0, t_0}\right) f(\bar{r}_2, 0 | \bar{r}_0, t_0) dr_2 \\
&+ \int_{t_0}^0 \int_C \phi_c(\bar{r}_b, t_b) \left(\frac{\partial}{\partial t_0} + L_{\bar{r}_0, t_0}\right) g(\bar{r}_b, t_b | \bar{r}_0, t_0) dr_b dt_b \\
&- \int_C \phi_c(\bar{r}_b, t_0) g(\bar{r}_b, t_0 | \bar{r}_0, t_0) dr_b
\end{aligned} \tag{3.5}$$

The right side of equation (3.5) is zero by Kolmogorov equations (2.23) and (2.26) and initial condition (2.4). Therefore,

$$-\frac{\partial \phi(\bar{r}_0, t_0)}{\partial t_0} = L_{\bar{r}_0, t_0} \phi(\bar{r}_0, t_0) \tag{3.1}$$

To prove that $\phi(\bar{r}_0, t_0)$ as defined by equation (3.4) also satisfies the initial and boundary conditions of Problem A, consider

$$\begin{aligned}
\lim_{t_0 \rightarrow 0} \phi(\bar{r}_0, t_0) &= \int_R \phi_0(\bar{r}_2) \lim_{t_0 \rightarrow 0} f(\bar{r}_2, 0 | \bar{r}_0, t_0) dr_2 \\
&+ \int_{t_0}^0 \int_C \phi_c(\bar{r}_b, t_b) \lim_{t_0 \rightarrow 0} g(\bar{r}_b, t_b | \bar{r}_0, t_0) dr_b dt_b \quad (3.6)
\end{aligned}$$

By equations (2.3) and (2.4), equation (3.6) becomes

$$\lim_{t_0 \rightarrow 0} \phi(\bar{r}_0, t_0) = \int_R \phi_0(\bar{r}_2) \delta(\bar{r}_2 - \bar{r}_0) dr_2 = \phi_0(\bar{r}_0) \quad (3.7)$$

$$\text{Therefore, } \phi(\bar{r}_0, 0) = \phi_0(\bar{r}_0). \quad (3.2)$$

Also,

$$\begin{aligned}
\lim_{\bar{r}_0 \rightarrow \bar{r}_b} \phi(\bar{r}_0, t_0) &= \int_R \phi_0(\bar{r}_2) \lim_{\bar{r}_0 \rightarrow \bar{r}_b} f(\bar{r}_2, 0 | \bar{r}_0, t_0) dr_2 \\
&+ \int_{t_0}^0 \int_C \phi_c(\bar{r}_b, t_b) \lim_{\bar{r}_0 \rightarrow \bar{r}_b} g(\bar{r}_b, t_b | \bar{r}_0, t_0) dr_b dt_b \quad (3.8)
\end{aligned}$$

By equations (2.5) and (2.6), this equation becomes

$$\begin{aligned} \lim_{\bar{r}_o \rightarrow \bar{r}_b} \phi(\bar{r}_o, t_o) &= \int_{t_o}^0 \int_C \phi_c(\bar{r}_b, t_b) \delta(\bar{r}_o - \bar{r}_b) \delta(t_b - t_o) dr_b dt_b \\ &= \phi_c(\bar{r}_o, t_o) . \end{aligned} \quad (3.9)$$

Therefore, $\phi(\bar{r}_b, t_o) = \phi_c(\bar{r}_b, t_o)$. (3.3)

Since all conditions of Problem A are satisfied, $\phi(\bar{r}_o, t_o)$ as defined by equation (3.4) is a solution of the problem.

The Monte Carlo solution of Problem A is obtained by approximating the expected value $\phi(\bar{r}_o, t_o)$ given by equation (3.4) with the average $\phi_N(\bar{r}_o, t_o)$ of the initial and boundary values ϕ_i that are recorded from a set of N random walks originating at (\bar{r}_o, t_o) . This average is

$$\phi_N(\bar{r}_o, t_o) = \frac{1}{N} \sum_{i=1}^N \phi_i \quad (3.10)$$

The convergence of $\phi_N(\bar{r}_o, t_o)$ to $\phi(\bar{r}_o, t_o)$ is considered in Section 3.5.

Problem B

Determine $\phi(\bar{r}_0, t_0)$ such that:

$$(1) \quad - \frac{\partial \phi(\bar{r}_0, t_0)}{\partial t_0} = L_{\bar{r}_0, t_0} \phi(\bar{r}_0, t_0) - d(\bar{r}_0, t_0) \phi(\bar{r}_0, t_0) \quad (3.11)$$

is satisfied within a bounded region R;

- (2) a piecewise continuous initial condition is satisfied within R; i.e.,

$$\phi(\bar{r}_0, 0) = \phi_0(\bar{r}_0); \quad (3.12)$$

- (3) a piecewise continuous boundary condition

$\phi_c(\bar{r}_b, t_0)$ is satisfied on the boundary C of R;
i.e.,

$$\phi(\bar{r}_b, t_0) = \phi_c(\bar{r}_b, t_0). \quad (3.13)$$

The statement of this problem is the same as that for Problem A except that ϕ satisfies the same partial differential equation as the auxiliary density functions u and v (Section 2.5). Therefore, by analogy with the previous problem, the solution is

$$\begin{aligned} \phi(\bar{r}_0, t_0) = & \int_R \phi_0(\bar{r}_2) u(\bar{r}_2, 0 | \bar{r}_0, t_0) dr_2 \\ & + \int_{t_0}^0 \int_C \phi_c(\bar{r}_b, t_b) v(\bar{r}_b, t_b | \bar{r}_0, t_0) dr_b dt_b. \end{aligned} \quad (3.14)$$

From definitions (2.54) and (2.55), equation (3.14) becomes

$$\begin{aligned}
 \phi(\bar{r}_0, t_0) &= \int_R \phi_0(\bar{r}_2) \left\langle \exp - \int_{t_0}^0 d[\bar{r}(t), t] dt \right\rangle \left. \begin{array}{l} \bar{r}(0) = \bar{r}_2 \\ \bar{r}(t_0) = \bar{r}_0 \end{array} \right. \\
 &+ \int_{t_0}^0 \int_C \phi_c(\bar{r}_b, t_b) \left\langle \exp - \int_{t_0}^{t_b} d[\bar{r}(t), t] dt \right\rangle \left. \begin{array}{l} \bar{r}(t_b) = \bar{r}_b \\ \bar{r}(t_0) = \bar{r}_0 \end{array} \right. \\
 &g(\bar{r}_b, t_b \mid \bar{r}_0, t_0) dr_b dt_b \tag{3.15}
 \end{aligned}$$

The expected value $\phi(\bar{r}_0, t_0)$ given by equation (3.15) can be approximated by the average $\phi_N(\bar{r}_0, t_0)$ of the product $\gamma_i \phi_i$ for N walks originating at (\bar{r}_0, t_0) where ϕ_i is the initial or boundary value at the terminal point of the i^{th} walk and γ_i is the value of

$$\gamma = \exp - \int_{t_0}^T d[\bar{r}(t), t] dt \tag{3.16}$$

for the corresponding walk. The upper limit of integration, \mathcal{T} , is 0 for walks terminating at $t = 0$, and t_b for walks terminating at a boundary. The Monte Carlo solution is therefore

$$\phi_N(\bar{r}_0, t_0) = \frac{1}{N} \sum_{i=1}^N \gamma_i \phi_i \quad (3.17)$$

3.3 Solutions of Boundary-Value Problems for Elliptic Partial Differential Equations

The boundary-value problems C, D and E to be discussed arise in the study of steady-state fields. Typical partial differential equations for these problems are the Laplace equation and the Poisson equation.

The statement of Problem C is as follows.

Problem C Determine $\phi(\bar{r}_0)$ such that:

$$(1) \quad L_{\bar{r}_0} \phi(\bar{r}_0) = 0 \text{ is satisfied within a bounded region } R; \quad (3.18)$$

region R;

$$(2) \quad \text{a piecewise continuous boundary condition } \phi_c(\bar{r}_b) \text{ is satisfied on the boundary } C \text{ of } R. \text{ i.e.,}$$

$$\phi(\bar{r}_b) = \phi_c(\bar{r}_b). \quad (3.19)$$

The subscript t_0 is deleted from operator $L_{\bar{r}_0, t_0}$

to indicate that $L_{\bar{r}_0}$ is independent of time.

The solution of this problem is the steady-state solution of a problem of type A. Since $L_{\bar{r}_0}$ and the boundary conditions are independent of t_0 , the solution at \bar{r}_0 is the expected value of boundary values at the terminal points of random walks originating at \bar{r}_0 at time $t_0 = 0$. The expected value is written in terms of probability density function $g(\bar{r}_b, t_b | \bar{r}_0, 0)$ as

$$\phi(\bar{r}_0) = \int_0^{\infty} \int_C \phi_c(\bar{r}_b) g(\bar{r}_b, t_b | \bar{r}_0, 0) dr_b dt_b \quad (3.20)$$

From equation (2.26) and boundary condition (2.6) for g , it follows that $\phi(\bar{r}_0)$ as given by equation (3.20) is indeed a solution of Problem C.

Equation (3.20) can also be written as

$$\phi(\bar{r}_0) = \int_C \phi_c(\bar{r}_b) G(\bar{r}_b | \bar{r}_0) dr_b \quad (3.21)$$

where

$$G(\bar{r}_b | \bar{r}_0) = \int_0^{\infty} g(\bar{r}_b, t_b | \bar{r}_0, 0) dt_b \quad (3.22)$$

is the probability density that a random walk starting at \bar{r}_0 at time $t_0 = 0$ will eventually terminate in dr_b on the boundary C . As for previous problems, the expected value given by equation (3.20) or (3.21) can be approximated by the average $\phi_N(\bar{r}_0)$ of the terminal boundary values ϕ_i . That is,

$$\phi_N(\bar{r}_0) = \frac{1}{N} \sum_{i=1}^N \phi_i \quad (3.23)$$

is the Monte Carlo solution.

Problem D

Determine $\phi(\bar{r}_0)$ such that:

$$(1) \quad L_{\bar{r}_0} \phi(\bar{r}_0) - d(\bar{r}_0)\phi(\bar{r}_0) = 0 \quad \text{within a} \quad (3.24)$$

bounded region R ;

(2) a piecewise continuous boundary condition

$\phi_c(\bar{r}_b)$ is satisfied on the boundary C of R ;

i.e.,

$$\phi(\bar{r}_b) = \phi_c(\bar{r}_b) \quad (3.25)$$

Operator $L_{\bar{r}_0}$ and coefficient $d(\bar{r}_0)$ are independent of

time t_0 , but otherwise are as defined by (2.24) and (2.56).

The solution of this problem is the steady-state solution of a problem of type B. Hence, by analogy with Problem C, the solution is

$$\phi(\bar{r}_0) = \int_0^\infty \int_C \phi_c(\bar{r}_b) v(\bar{r}_b, t_b | \bar{r}_0, 0) dr_b dt_b \quad (3.26)$$

For a large number N of random walks starting from \bar{r}_0 at time $t_0 = 0$, the expected value $\phi(\bar{r}_0)$ can be approximated by

$$\phi_N(\bar{r}_0) = \frac{1}{N} \sum_{i=1}^N \gamma_i \phi_i \quad (3.27)$$

where γ_i is the value of $\gamma = \exp - \int_{t_0}^{t_b} d[\bar{r}(t)] dt$

for the i^{th} walk and ϕ_i is the boundary value at the terminal point of the i^{th} walk.

3.4 Solutions of Nonhomogeneous Boundary-Value Problems

The solutions of nonhomogeneous boundary-value problems can be constructed from the solutions of a homogeneous time-independent boundary-value problem and a homogeneous time-dependent boundary-value problem. Poisson's equation is a typical example for problems of type E. The statement of Problem E is as follows.

Problem E Determine $\phi(\bar{r}_0)$ such that:

$$(1) \quad L_{\bar{r}_0} \phi(\bar{r}_0) = -H(\bar{r}_0) \text{ is satisfied within a} \quad (3.28)$$

bounded region R , where $H(\bar{r}_0)$ is a piecewise continuous function;

$$(2) \quad \text{a piecewise continuous boundary condition } \phi_c(\bar{r}_b)$$

is satisfied on the boundary C of R; i.e.,

$$\phi(\bar{r}_b) = \phi_c(\bar{r}_b) . \quad (3.29)$$

To determine the solution of Problem E, consider the time-independent boundary-value problem of type C:

$$(1) \quad L_{\bar{r}_o} \phi_1(\bar{r}_o) = 0 \text{ within } R, \quad (3.30)$$

$$(2) \quad \phi_1(\bar{r}_b) = \phi_c(\bar{r}_b) \text{ on the boundary } C \text{ of } R; \quad (3.31)$$

and the time-dependent boundary-value problem of type A:

$$(1) \quad - \frac{\partial}{\partial t_o} \phi_2(\bar{r}_o, t_o) = L_{\bar{r}_o} \phi_2(\bar{r}_o, t_o) \text{ within } R, \quad (3.32)$$

$$(2) \quad \phi_2(\bar{r}_o, 0) = H(\bar{r}_o) \quad (3.33)$$

$$(3) \quad \phi_2(\bar{r}_b, t_o) = 0 . \quad (3.34)$$

The solution of Problem E is given by

$$\phi(\bar{r}_o) = \phi_1(\bar{r}_o) + \int_{-\infty}^0 \phi_2(\bar{r}_o, t_o) dt_o . \quad (3.35)$$

Proof Operate on $\phi(\bar{r}_o)$ with $L_{\bar{r}_o}$ and use (3.30) and (3.32).

$$L_{\bar{r}_o} \phi(\bar{r}_o) = - \int_{-\infty}^0 \frac{\partial}{\partial t_o} \phi_2(\bar{r}_o, t_o) dt_o \quad (3.36)$$

$$= \phi_2(\bar{r}_o, -\infty) - \phi_2(\bar{r}_o, 0) . \quad (3.37)$$

Since the boundary values for ϕ_2 are 0, $\phi_2(r_0, -\infty) = 0$.

Therefore, by (3.33),

$$L_{\bar{r}_0} \phi(\bar{r}_0) = -H(\bar{r}_0) \quad (3.28)$$

From (3.35), for $\bar{r}_0 = \bar{r}_b$,

$$\phi(\bar{r}_b) = \phi_1(\bar{r}_b) + \int_{-\infty}^0 \phi_2(\bar{r}_b, t_0) dt_0 \quad (3.38)$$

Therefore, by conditions (3.31) and (3.34),

$$\phi(\bar{r}_b) = \phi_c(\bar{r}_b) \quad (3.29)$$

The solution $\phi(\bar{r}_0)$ given by (3.35) satisfies all conditions of Problem E, and is therefore a solution.

The Monte Carlo solution of Problem E is obtained by determining $\phi_1(\bar{r}_0)$ and $\phi_2(\bar{r}_0, t_0)$ by the methods of Problems A and C and then integrating $\phi_2(\bar{r}_0, t_0)$ with respect to t_0 by some numerical technique.

Nonhomogeneous equations of the form

$$L_{\bar{r}_0} \phi(\bar{r}_0) - d(\bar{r}_0)\phi(\bar{r}_0) = -H(\bar{r}_0) \quad (3.39)$$

are solved in the same manner as Problem E by considering problems of type B and D.

3.5. Estimates of the Number of Random Walks for Monte Carlo Solutions

3.5A Convergence of Monte Carlo Solutions

Monte Carlo solutions of homogeneous partial differential equations are given by

$$\phi_N(r_o, t_o) = \frac{1}{N} \sum_{i=1}^N \phi_i$$

where for problems of type B and D, ϕ_i is replaced by $\gamma_i \phi_i$. Let the recorded values ϕ_i , for a given (\bar{r}_o, t_o) be denoted by the random variable ϕ . The variance of $\phi_N(\bar{r}_o, t_o)$, which is a measure of the fluctuations of values of $\phi_N(\bar{r}_o, t_o)$ obtained on different trials, is given by

$$\text{var } \phi_N(r_o, t_o) = \frac{1}{N} \text{var } \phi \quad (3.40)$$

From the Central Limit Theorem, $\phi_N(\bar{r}_o, t_o)$ will be nearly normally distributed for N large. It therefore follows that the probability is approximately .05 that

$$\left| \phi_N(\bar{r}_o, t_o) - \phi(\bar{r}_o, t_o) \right| > 2 \sqrt{\frac{\text{var } \phi}{N}} \quad (3.41)$$

Hence, the statistical convergence of $\phi_N(\bar{r}_o, t_o)$ to $\phi(\bar{r}_o, t_o)$

is as $\frac{1}{\sqrt{N}}$. To reduce the standard deviation $\sqrt{\text{var } \phi_N(\bar{r}_o, t_o)}$

by a factor of 2, for example, it is necessary to simulate 4N random walks.

3.5B Number of Random Walks for Homogeneous Partial Differential Equations

An estimate of the number N of random walks that are required for a given tolerable error can be determined as follows. If an error $\left| \phi_N(\bar{r}_0, t_0) - \phi(\bar{r}_0, t_0) \right|$ greater than ϵ , occurring with probability .05, is tolerable, then from inequality (3.41)

$$N > \frac{4 \text{ var } \phi}{\epsilon^2} \quad (3.42)$$

is a sufficient number of random walks. For some special cases, $\text{var } \phi$ can be calculated, so that for these cases condition (3.42) gives a lower bound for N . When $\text{var } \phi$ cannot be calculated, an estimate for N can be obtained by noting that

$$\text{var } \phi \leq \phi_{\max}^2 \quad (3.43)$$

where ϕ_{\max} is the maximum value of ϕ . A pessimistic estimate of the required number of random walks is therefore

$$N > \frac{4\phi_{\max}^2}{\epsilon^2} \quad (3.44)$$

For example, if the partial differential equation is scaled so that $\phi_{\max} = 1$, then for $\epsilon = .05$, N should be greater than 1,600; whereas if $\epsilon = .01$, then N should be greater than 40,000.

3.5C Number of Random Walks for Nonhomogeneous Partial Differential Equations.

The solution of nonhomogeneous partial differential equations of type E is given by

$$\phi(\bar{r}_0) = \phi_1(\bar{r}_0) + \int_{-\infty}^0 \phi_2(\bar{r}_0, t_0) dt_0 \quad (3.35)$$

For a Monte Carlo solution, $\phi_1(\bar{r}_0)$ is approximated by $\phi_{1N}(\bar{r}_0)$ and the integral is approximated by

$$I = \sum_{i=1}^M \alpha_i \phi_{2L}(\bar{r}_0, i \Delta t_0) \quad (3.45)$$

where the α_i depend upon the numerical integration that is used. The subscript L indicates that each value of $\phi_2(\bar{r}_0, t_0)$ is to be obtained using L random walks. The selection of numbers N and L will now be considered. Let the Monte Carlo approximation to $\phi(\bar{r}_0)$ be denoted by $\phi_{NL}(\bar{r}_0)$, then

$$\text{var } \phi_{NL}(\bar{r}_0) = \text{var } \phi_{1N}(\bar{r}_0) + \sum_{i=1}^M \alpha_i^2 \text{var } \phi_{2L}(\bar{r}_0, i \Delta t_0) \quad (3.46)$$

If $\text{var } \phi_{2L}(\bar{r}_o, j \Delta t_o)$ is the maximum value of $\text{var } \phi_{2L}(\bar{r}_o, i, \Delta t_o)$,
 $i = 1, \dots, M$, and if α_i are chosen by the trapezoidal rule;
 i.e.,

$$\alpha_1 = \alpha_M = \frac{\Delta t_o}{2} \quad (3.47)$$

$$\alpha_i = \Delta t_o \quad i = 2, 3, \dots, (M-1)$$

then

$$\text{var } \phi_{NL}(\bar{r}_o) \leq \text{var } \phi_{1N}(\bar{r}_o) + \text{var } \phi_{2L}(\bar{r}_o, j \Delta t_o) (\Delta t_o)^2 (M - \frac{3}{2}) \quad (3.48)$$

Let ϕ_1 and ϕ_2 be the random variables from which $\phi_{1N}(\bar{r}_o)$ and
 $\phi_{2L}(\bar{r}_o, j \Delta t_o)$ are formed; then

$$\text{var } \phi_{1N}(\bar{r}_o) = \frac{\text{var } \phi_1}{N} \leq \frac{\phi_c^2 \max}{N} \quad (3.49)$$

$$\text{var } \phi_{2L}(\bar{r}_o, j \Delta t_o) = \frac{\text{var } \phi_2}{L} \leq \frac{H_{\max}^2}{L} \quad (3.50)$$

$\phi_c \max$ and $H_c \max$ are the maximum absolute values of the boundary
 function $\phi_c(\bar{r}_b)$ and function $H(\bar{r}_o)$, respectively, for the problem.
 It therefore follows that

$$\text{var } \phi_{NL}(\bar{r}_o) \leq \frac{\phi_c^2 \max}{N} + \frac{H_{\max}^2}{L} (\Delta t_o)^2 (M - \frac{3}{2}) \quad (3.51)$$

The numbers N and L can be chosen to minimize the right-hand
 side of this expression subject to the constraint $N+ML = Q$,
 where Q is the total number of random walks that are taken to

obtain a value of $\phi(\bar{r}_0)$. The minimization gives

$$L = N(\Delta t_0) \sqrt{\frac{M - \frac{3}{2}}{M}} \left(\frac{H_{\max}}{\phi_{c \max}} \right)^2 \quad (3.52)$$

This results, when used with the Poisson equation in Section 5.4, gave $L = 133$ for $N = 1,000$ and $M = 19$. Thus, at least for this example, the time required to obtain a Monte Carlo value of the integral I was only about twice the time required to obtain a value of $\phi_{1N}(\bar{r}_0)$.

4. COMPUTER MECHANIZATION OF MONTE CARLO METHODS FOR SOLVING PARTIAL DIFFERENTIAL EQUATIONS

4.1 Introduction

Based upon the equations given in Chapters 2 and 3 for the Monte Carlo solutions of partial differential equations, a computing system for implementing the methods must perform the following operations.

1. The stochastic differential equations of Section 2.4, namely

$$\frac{dx}{dt} + A_1(x, y, z, t) = B_1(x, y, z, t)N_1(t) \quad (2.27)$$

$$\frac{dy}{dt} + A_2(x, y, z, t) = B_2(x, y, z, t)N_2(t) \quad (2.28)$$

$$\frac{dz}{dt} + A_3(x, y, z, t) = B_3(x, y, z, t)N_3(t) \quad (2.29)$$

with initial conditions $\bar{r}(t_0) = \bar{r}_0$ must be simulated. In addition, for partial differential equations that contain ϕ itself, the functional

$$\gamma = \exp - \int_{t_0}^T d[\bar{r}(t), t] dt \quad (3.16)$$

must be generated.

2. The stochastic process must be terminated either at time $t = 0$ or whenever the boundary C of a region R is reached. This requires a method for storing and detecting boundaries.
3. The initial or boundary values ϕ_i at the terminal points of the random walks must be generated.
4. The average

$$\phi_N(\bar{r}_0, t_0) = \frac{1}{N} \sum_{i=1}^N \phi_i$$

or

$$\phi_N(\bar{r}_0, t_0) = \frac{1}{N} \sum_{i=1}^N \gamma_i \phi_i$$

for N very large must be obtained at each point (\bar{r}_0, t_0) for which a solution is desired.

5. The stochastic process must be initiated, terminated and reset for each random walk. Automatic readout of $\phi_N(\bar{r}_0, t_0)$ and adjustment of (\bar{r}_0, t_0) after each set of N random walks is also desirable.

In this chapter a computing system in which operations 1, 2 and 3 are carried out by an analog computer and operations 4 and 5 are carried out by an associated digital computer will be described.

The experimental studies were carried out on an Electronics Associates Inc. PACE 231 R-V analog computer and a Logistics Research ALWAC III-E digital computer. The design

and construction of interface equipment for hybridizing the two computers was an integral part of the project. Details of this aspect of the work appear in the literature⁸ and in Appendix I.

4.2 Simulation of the Stochastic Process on an Analog Computer

4.2A Analog Computer Setup

In the proposed Monte Carlo methods, the general stochastic process defined by differential equations (2.27) to (2.29) is simulated on the analog computer. These differential equations are of first order, and in general they are coupled, nonlinear and nonautonomous. For many partial differential equations of engineering importance, however, the stochastic differential equations reduce to independent, linear autonomous form. The stochastic equations for Laplace's equation, $\nabla^2 \phi = 0$, and the heat equation, $\nabla^2 \phi = \frac{\partial \phi}{\partial t}$, for example, only involve integration of the noise terms $N_i(t)$.

An analog computer block diagram for simulating the stochastic differential equation (2.27) in its most general form is shown in Figure 4-1. The function generation indicated in this figure can be realized simply with diode function generators and quarter-square multipliers whenever closed-form mathematical expressions are known for the functions or whenever the functions are of only a single variable. Special techniques¹³ are required for generation of functions of a more general form.

Integrator A2 shown in Figure 4-1 is used to "track and hold" the random variable x . This track-and-hold feature is used

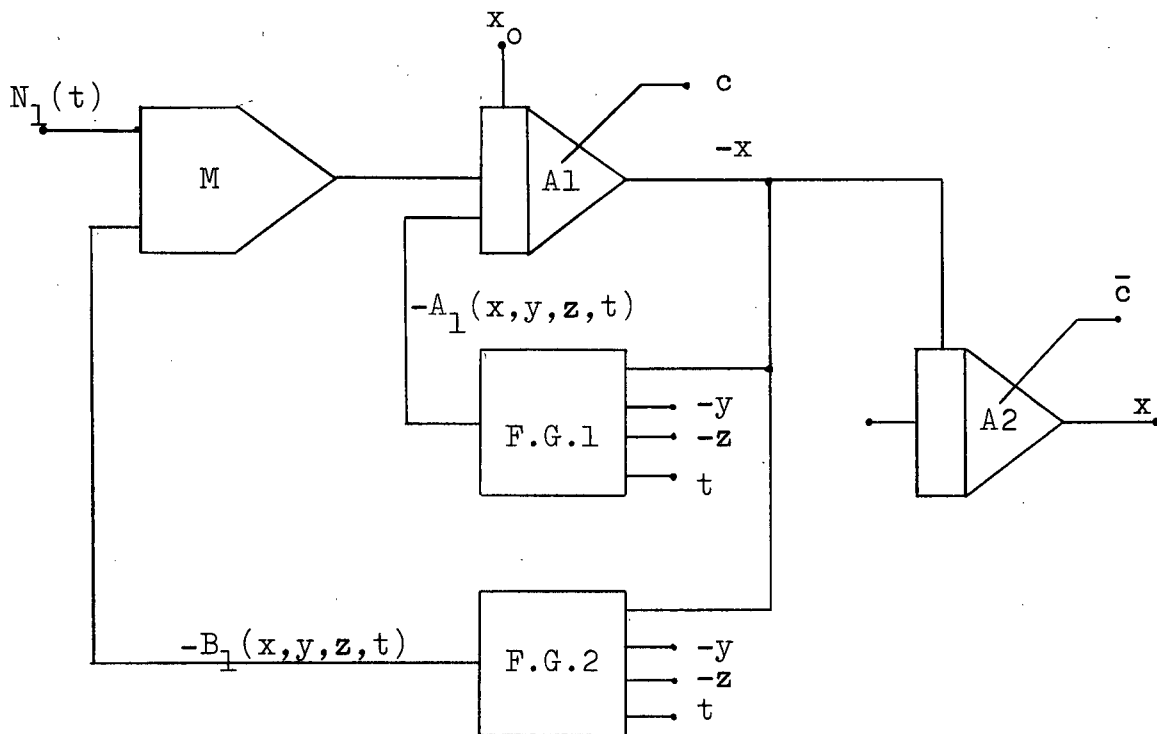


Figure 4-1. Block Diagram for Simulation of a Stochastic Differential Equation

to hold the terminal value of the random vector \bar{r} , and consequently the initial or boundary value ϕ_i generated from \bar{r} , (Section 4.4) at a constant value while ϕ_i or $(\gamma_i \phi_i)$ is read by the digital computer. The mode-control signal c and its logical inverse \bar{c} synchronize the track-and-hold modes of integrator A2 with the compute and initial-condition modes respectively of integrator A1. The generation of these mode-control signals from electronic comparators and the digital computer is discussed in Section 4.3.

For problems in which the functional γ must be generated,

the following implicit method is used. From equation (3.16),

$$\frac{d\gamma}{dt} = -\gamma d[\bar{r}(t), t] \quad (4.1)$$

and

$$\gamma(t_0) = 1$$

An analog computer block diagram for these equations is shown in Figure 4-2. γ is available at the output of integrator A3. Note that the mode of integrator A3 is also controlled by c .

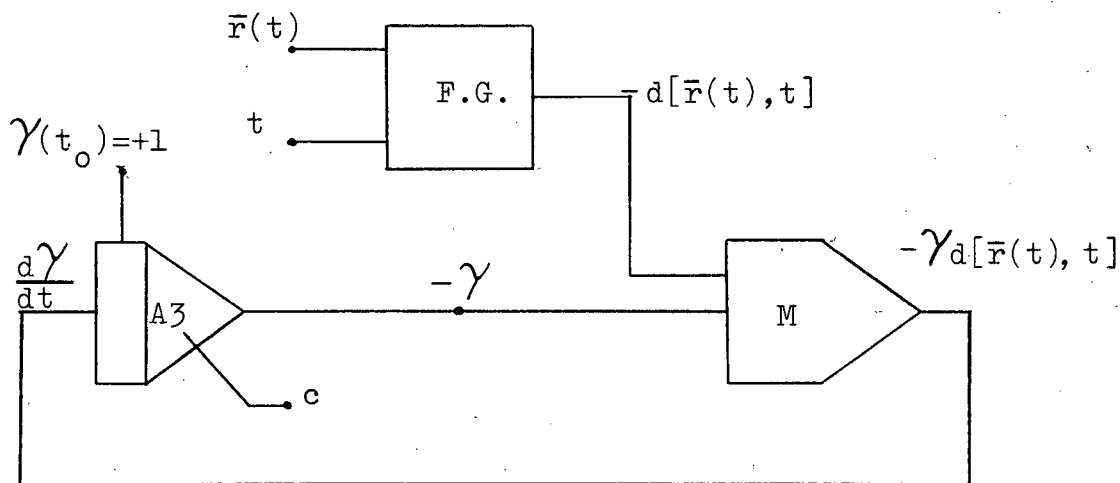


Figure 4-2. Block Diagram for Generation of γ .

4.2B. Noise Source Requirements

The uncorrelated Gaussian white noise specified in the theory (Section 2.4) must be approximated by noise sources that are physically realizable. Noise sources with approximately Gaussian distributions but with limited bandwidth ω_N can be derived from gas tubes, pseudo-random number generators¹⁴ etc. If the noise bandwidth ω_N is larger than the bandwidth capabilities of the analog computer, then it can be assumed that any errors resulting from finite bandwidths are caused by the analog computer and not the noise sources. In the case of a PACE 231 R-V analog computer, ω_N should be larger than 10^5 radians/sec. to be above the bandwidth capabilities of the computer. The effect of a limited-bandwidth amplifier within the analog computer is considered in Section 4.2 C.

In addition to the bandwidth requirements, the statistics of the noise sources must be stationary during the complete problem solving time which for some problems could be several hours. Without special precautions, many commercially available noise sources fail to meet this requirement.⁴

To overcome noise-source bandwidth and stability limitations that were encountered in this study, the multichannel noise source described in Appendix II was developed.⁹ This noise source produces stable discrete-interval binary noise with levels ± 5.0 volts, and has an adjustable bandwidth that can exceed the bandwidth of the analog computing elements. Approximately Gaussian distributed noise can be obtained from this noise source by low-pass filtering the binary noise.¹⁴ It was found in the

experimental study, however, that good Monte Carlo solutions could be obtained by using the binary noise directly. For good results, the step size of the response must be extremely small compared to the size of the region R. Under this condition, the change in $\bar{r}(t)$ during a small time Δt is small, so that the assumptions made in Section 2.4 are approximated.

Some inherent advantages result from the use of binary noise. One, the statistical properties of the noise are known precisely and can be checked easily. Two, the discrete nature of the response is helpful in scaling the stochastic differential equations since the response can be monitored on an oscilloscope, and the scaling adjusted until the step size is extremely small compared to the size of the region R.

4.2C. Effect of Finite Bandwidths on Solution Times

In theory, if infinite-bandwidth noise and analog computing elements (amplifiers etc.) were realizable, it would be possible to time scale the stochastic differential equation to obtain random walks at an arbitrarily high rate. Some insight into time-scaling limitations due to finite bandwidths is obtained by the following means. Assume all computing elements and the noise source shown in Figure 4-1 are ideal except integrator A1. Let integrator A1 have the transfer function¹⁵

$$T(s) = - \frac{a}{s} \left(\frac{\omega_0}{s + \omega_0} \right) \quad (4.2)$$

where ω_0 is a measure of the bandwidth of the amplifier, and a

is a time-scaling factor (gain). Under these assumptions, the computer variable x satisfies the following differential equation:

$$\left(\frac{\alpha}{\omega_0}\right) \frac{d^2x}{d\tau^2} + \frac{dx}{d\tau} + A_1(x,y,z,\tau) = B_1(x,y,z,\tau)N_1(\tau) \quad (4.3)$$

where $\tau = \alpha t$ is the scaled-time variable. For the statistics of the computer variable x to closely approximate the statistics of the response to stochastic differential equation (2.27), the effect of the second derivative term must be negligible. Hence, to minimize error α should be kept small, but to reduce solution time α should be made large. The compromise that must be made in choosing α can best be determined experimentally. This is done by increasing α until experimental values of the solution of the partial differential equation deviate from solutions obtained with α small. By checking at several points, the largest value of α for good results can be ascertained.

4.3 Detection of Boundaries

An analog computer simulation of the stochastic differential equations for the random vector \bar{r} was discussed in the previous section. In this section, methods will be outlined for terminating the stochastic process at a given time $t = 0$ or whenever \bar{r} reaches a boundary C of a region R . The methods given are novel in that only electronic comparators and diode function generators are required. Hence, special purpose equipment such as an oscilloscope mask and a phototube detector⁴ is not required.

Upon the detection of a boundary or at $t = 0$, the mode-control signal c must be reversed in order to place all integrators in the initial-condition mode. Since the track-and-hold amplifiers are controlled by \bar{c} , the reversal of c places these amplifiers in the hold mode. In this state, the boundary point \bar{r}_b on C , or terminal point $\bar{r}(0)$ is held fixed while a terminal value ϕ_i or $\gamma_i \phi_i$ is transferred to the digital computer. Immediately after the transfer to the digital computer, c is reversed by the digital computer, and a new random walk is initiated.

The mode-control signals c and \bar{c} are conveniently generated from a mode-control flip-flop that can be triggered from electronic comparators on the analog computer or from a pulse from the digital computer. The triggering scheme for the mode-control flip-flop is shown in Figure 4-3.

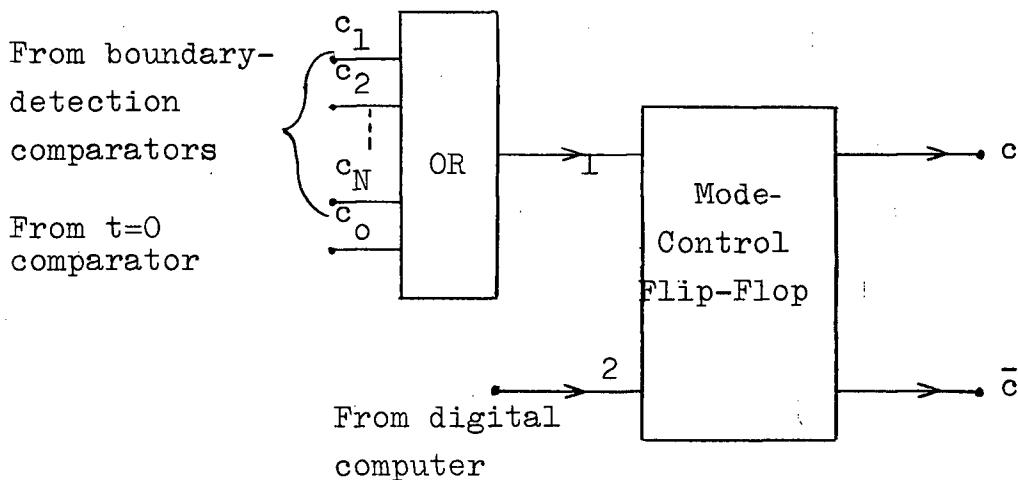


Figure 4-3. Triggering of Mode-Control Flip-Flop

A pulse at input (1) terminates a simulation of the stochastic differential equations, and a pulse at input (2) initiates a new simulation of the equations. With this scheme, the problem of detecting boundaries and time $t = 0$ is reduced to the problem of energizing electronic comparators whenever a boundary is reached or whenever $t = 0$.

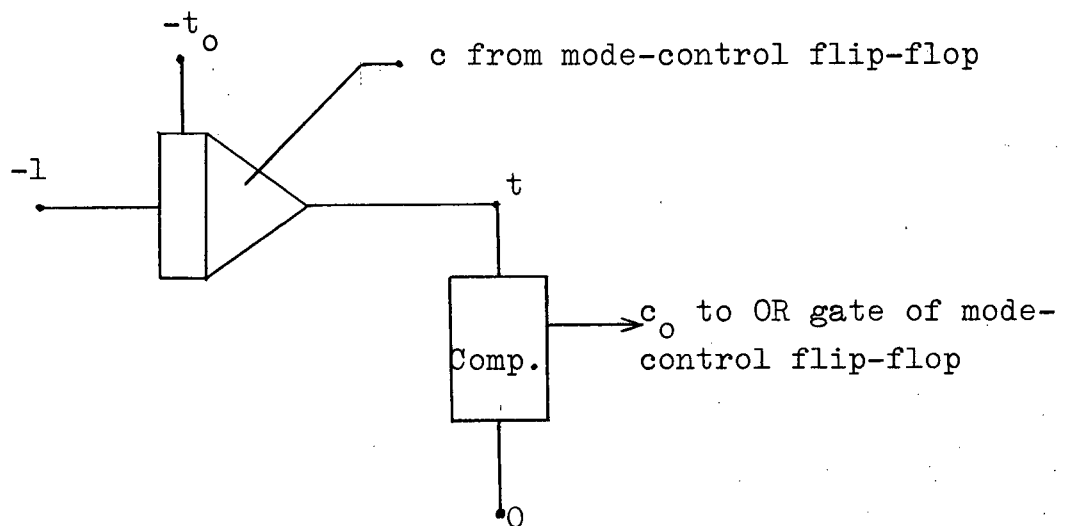


Figure 4-4. Detection of Termination Time $t = 0$

The use of an electronic comparator to detect time $t = 0$ for random walks starting at time t_0 is shown in Figure 4-4. A signal c_0 is obtained from the comparator when $t = 0$. Note that c controls the mode of the integrator that is shown in this figure. Hence, this integrator is placed in the initial-condition mode at $t = 0$ or when a boundary is reached, and in the compute mode at $t = t_0$.

4.3A Detection of Boundaries for Problems with One Space Variable

For problems with one space variable x , and boundaries at points x_{b1} and x_{b2} , the boundary detection comparators are energized by comparing the random voltage x with voltages x_{b1} and x_{b2} . (see Figure 4-5).

from analog
circuit simulating
the stochastic
differential equations

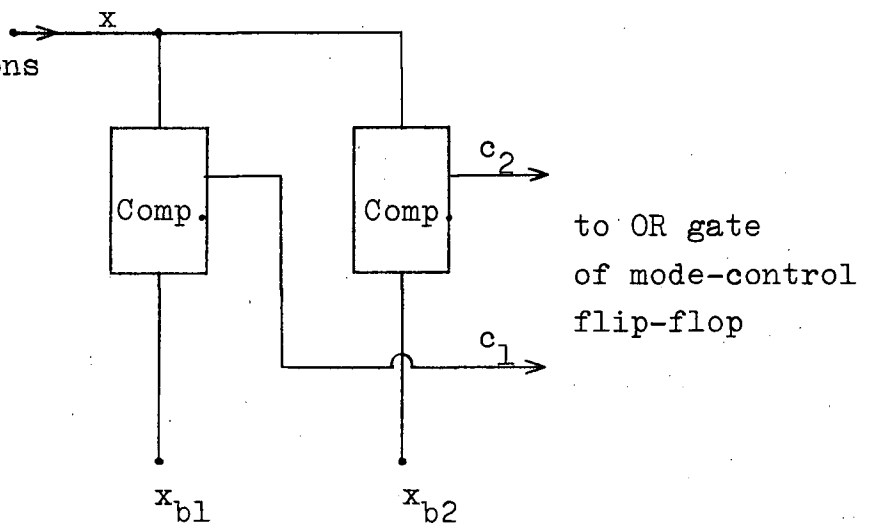


Figure 4-5. Boundary Detection for Problems with One Space Variable.

When x reaches x_{b1} or x_{b2} , the mode-control flip-flop is triggered by either comparator output c_1 or c_2 .

4.3B Detection of Boundaries for Problems with Two Space Variables

Consider first the simple two-dimensional region R with boundary C as shown in Figure 4-6.

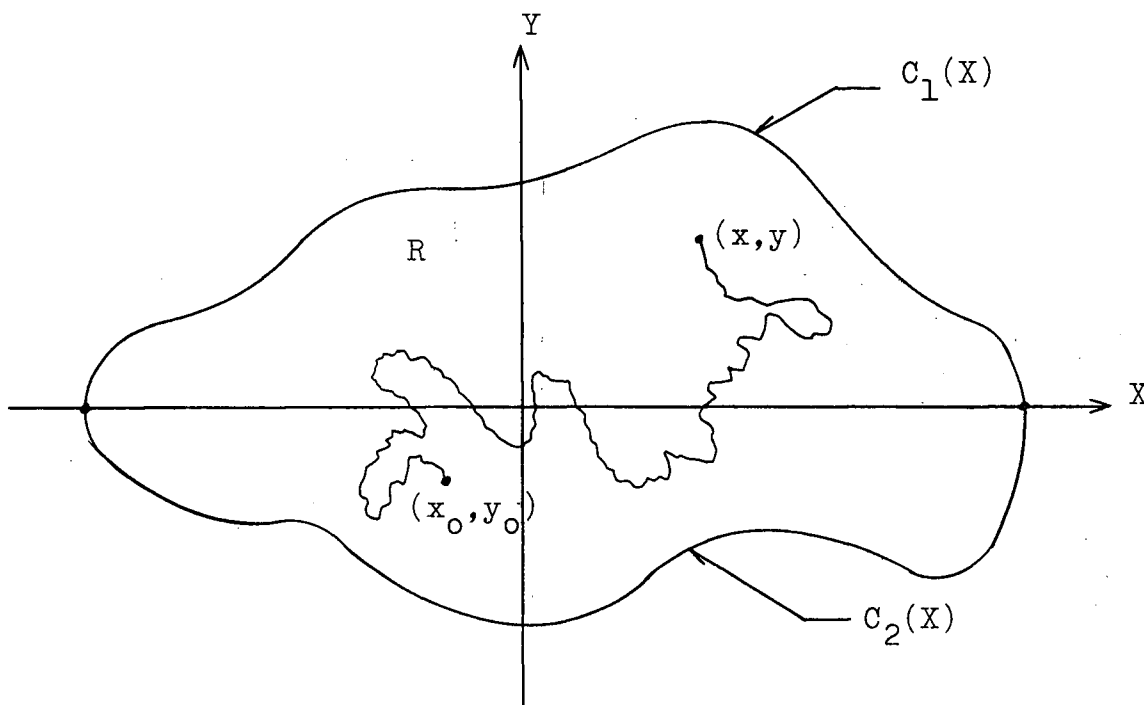


Figure 4-6. Two-Dimensional Region

The boundary of this region is composed of two curves $C_1 = C_1(X)$ and $C_2 = C_2(X)$, each of which is a single-valued function of X . A typical random walk with instantaneous components (x, y) is also shown in the figure.

It is clear from Figure 4-6 that a random walk reaches a boundary whenever

$$y = C_1(x)$$

(4.4)

or

$$y = C_2(x)$$

This boundary detection criterion is implemented on the analog computer by comparing the random variable y with functions $C_1(x)$ and $C_2(x)$ that are set on diode function generators. A block diagram of this simple boundary detection scheme is shown in Figure 4-7.

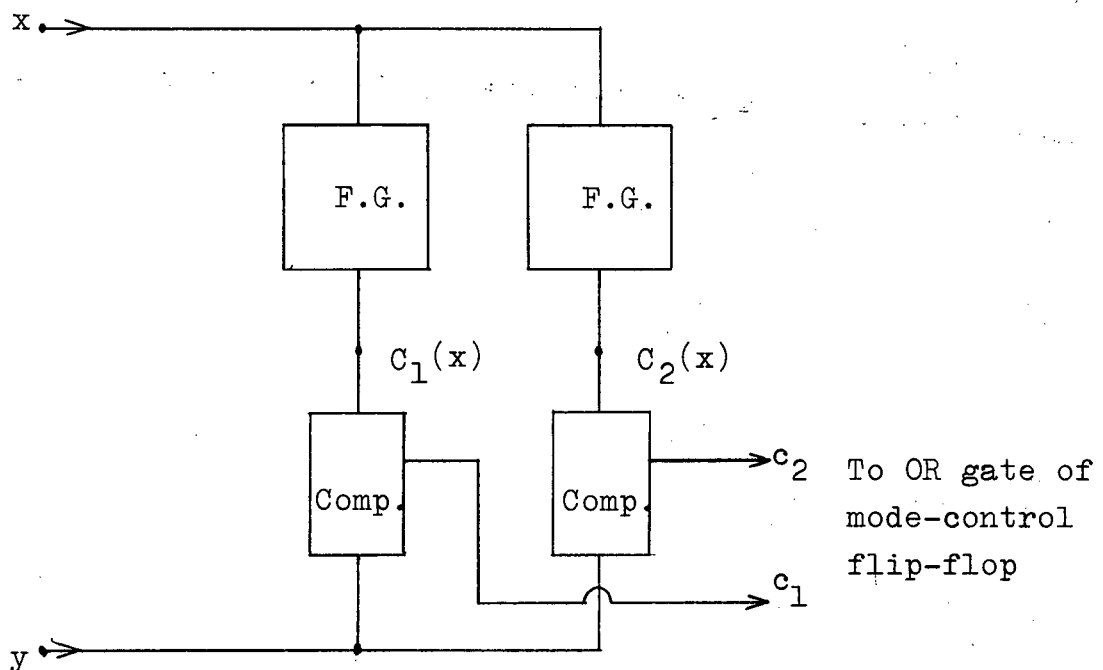


Figure 4-7. Two-Dimensional Boundary Detection

Now consider a more general region R in which a dividing line D can be constructed such that C_1 and C_2 are single-valued functions of U measured along D . (see Figure 4-8). This type of region will be called a simple region. The region considered previously in which U was coincident with X , is a special case of a simple region.

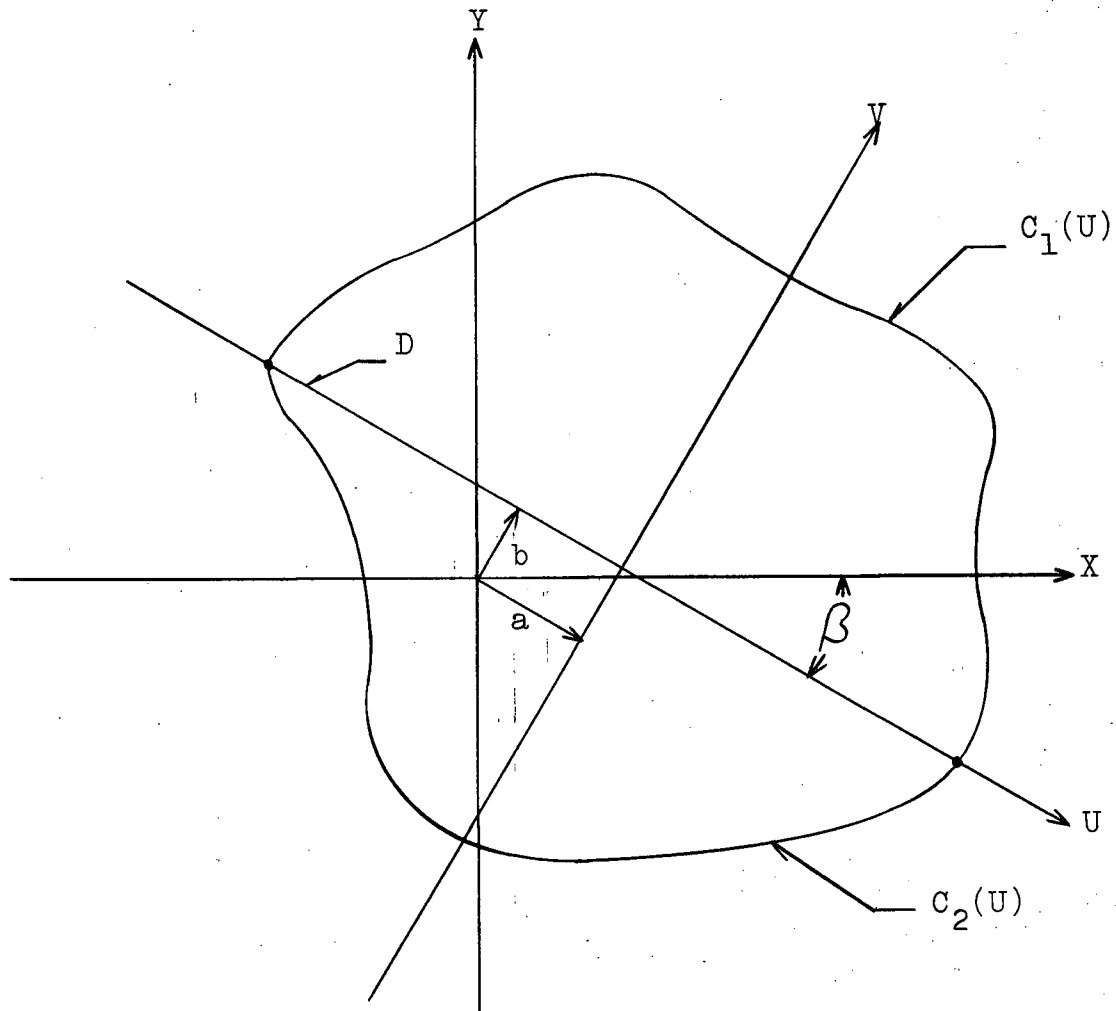


Figure 4-8. Coordinate Transformation used for Boundary Detection of Two-Dimensional Simple Regions.

The boundaries of an arbitrary simple region are detected by transforming the random variables x and y to new variables u and v for which the boundary detection equations

$$v = C_1(u) \tag{4.5}$$

and $v = C_2(u)$

can be used. The new variables u and v are obtained from x

and y by the transformation

$$\begin{aligned} u &= x \cos \beta - y \sin \beta - a \\ v &= x \sin \beta + y \cos \beta - b \end{aligned} \quad (4.6)$$

where constants a , b and β are defined in Figure 4-8. Hence, to detect this type of boundary, variables u and v instead of x and y , respectively, are used with the boundary detection scheme of Figure 4-7.

For more complicated regions R in which a dividing line D cannot be found, the region is divided into two or more simple regions R_1, R_2, \dots , and the exit of the random variable \bar{r} from each simple region is detected by the method given. By combining the signals obtained from each simple region with an AND gate, a signal is obtained when \bar{r} leaves all the simple regions R_i and hence the region R .

In many engineering problems the boundaries are described by a simple mathematical expression. When this is the case, the boundaries can be detected by an even simpler method than that given above. Consider, for example, an elliptical boundary C defined by the equation

$$\frac{(X + a)^2}{b^2} + \frac{(Y + c)^2}{d^2} = 1 \quad .$$

The function

$$f(x,y) = \frac{(x+a)^2}{b^2} + \frac{(y+c)^2}{d^2}$$

is generated with multipliers from the random variables x and y , and compared to 1. Whenever $f(x,y) = 1$ the random walk is at the boundary. Hence, only two multipliers and one comparator are required to detect this type of boundary. Since the parameters a , b , c and d of the elliptical region can be varied simply by adjusting an analog voltage, problems in which a solution is desired at some point, as a function of the parameters, can be handled easily. (see example of Section 5.3).

The versatility of the boundary detection methods that have been proposed is evident from the photograph shown in Figure 4-9. This photograph of a circular region within a simple region was taken by continuously exposing an oscilloscope display with the vertical axis driven by random variable y and the horizontal axis driven by random variable x . The random walks (not visible) for this photograph were started at points uniformly distributed on a circle between the boundaries of the two regions. A dot was produced at the termination point of each random walk.

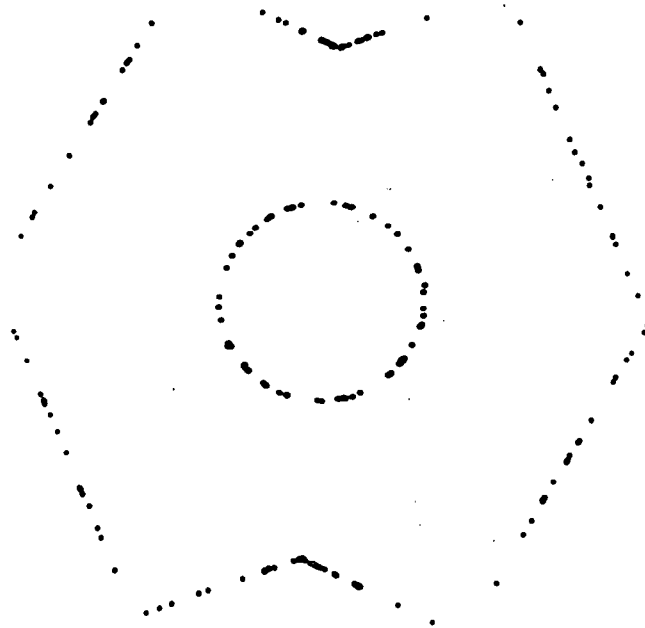


Figure 4-9. Photograph Illustrating a Detected Boundary

4.3C Detection of Boundaries for Problems with Three Space Variables

The dividing-line method discussed in Section 4.3B can be generalized to three-dimensional regions by using a dividing plane such that the boundary surface above and below the plane is a single-valued function of position on the plane. For regions in which simple mathematical expressions are known for the functions of two variables that define the surface above and below the dividing plane, this method is easy to apply. If this is not the case, however, special purpose function generation techniques¹³ would have to be used.

The boundaries of three-dimensional regions with some type of symmetry can often be detected by combining the methods described for one- and two-dimensional regions. For example, the cubic region of Section 5.6 is detected by using 3 pairs of comparators in the same manner that a single pair is used for one-dimensional problems. In addition, boundaries that can be defined with a single expression, for example ellipsoids, can be detected in the same manner as corresponding boundaries in two dimensions.

4.4 Generation of Initial and Boundary Values

At the instant the terminal time $t = 0$ or a boundary C is reached, the mode-control flip-flop is triggered from a comparator by the methods that have been discussed. The triggering of this flip-flop places the track-and-hold amplifiers (Figure 4-1) in the hold mode so that the terminal values of the components x , y , and z of \bar{r} are available as constant voltages on the analog computer. The initial and boundary values ϕ_i are generated with function generators from these components of \bar{r} .

The function generation prescribed above can be carried out with function generators and multipliers whenever the initial and/or boundary values are known as simple functions of x , y and z or whenever they can be expressed as a function of a single variable. For two-dimensional problems in which a dividing line D is used for detecting the boundaries, the boundary values are conveniently generated as a function of

the variable u defined along the dividing line.

When the values ϕ_i cannot be generated conveniently by analog computer techniques, they can always be generated within the digital computer. When the digital computer is used for function generation, the components x , y and z of the terminal position vector $\bar{r}(0)$ or \bar{r}_b are read; then a table stored within the computer is scanned, or some other method is used, to determine the corresponding value of ϕ_i . Since more than one value must be read by the digital computer and since additional digital operations are required, this procedure with slow digital equipment is more time consuming than analog function generation. However, with fast digital equipment it is possible to store the terminal components x , y and z of the i^{th} walk with a track-and-hold arrangement and read them during the $(i + 1)^{\text{st}}$ walk. Thus, if the conversion equipment and digital computer are sufficiently fast, the values x , y and z can be read and the digital function generation for the i^{th} walk can be carried out while the analog computer is simulating the $(i + 1)^{\text{st}}$ random walk. This procedure is very efficient in that essentially no time is wasted between walks.

For problems in which voltages from more than one location within the analog computer must be read by the digital computer, a gating arrangement is often necessary for multiplexing to a single analog-to-digital converter. By suitably patching an EAI amplifier equipped with electronic switching, an electronic SPDT switch that is suitable for this purpose can be realized. This switch is described in Appendix III.

4.5 Operations Performed by the Digital Computer

The terminal values ϕ_i (or $\gamma_i\phi_i$) for each random walk are generated by the techniques that have been described. The main function of the digital computer is to compute the average of the terminal values and to control the analog computer during the complete problem solving time.

The average $\phi_N(\bar{r}_0, t_0)$ for each point (\bar{r}_0, t_0) at which a solution is desired is formed by adding, in sequence, each value ϕ_i (or $\gamma_i\phi_i$) to a partial sum stored within the digital computer. A tally of the number of random walks that have been completed is kept by the digital computer, and after N walks the average is typed out. A digital computer, or at least a digital method, is necessary for this operation because for N large (1,000 - 40,000), an extremely large dynamic range is required to obtain the sum precisely.

The control functions performed by the digital computer are carried out through the mode-control flip-flop (Section 4-3) and by a group of logic lines (flags) running from the digital computer to the memory and logic unit of the analog computer. These logic lines control electronic switches and relays that are used for multiplexing, and other switching operations on the analog computer.

The complete hybrid system for implementing the Monte Carlo methods is shown in Figure 4-10. Voltage levels on the analog computer are converted to binary-coded decimal form by the analog-to-digital converter of the EAI digital voltmeter.

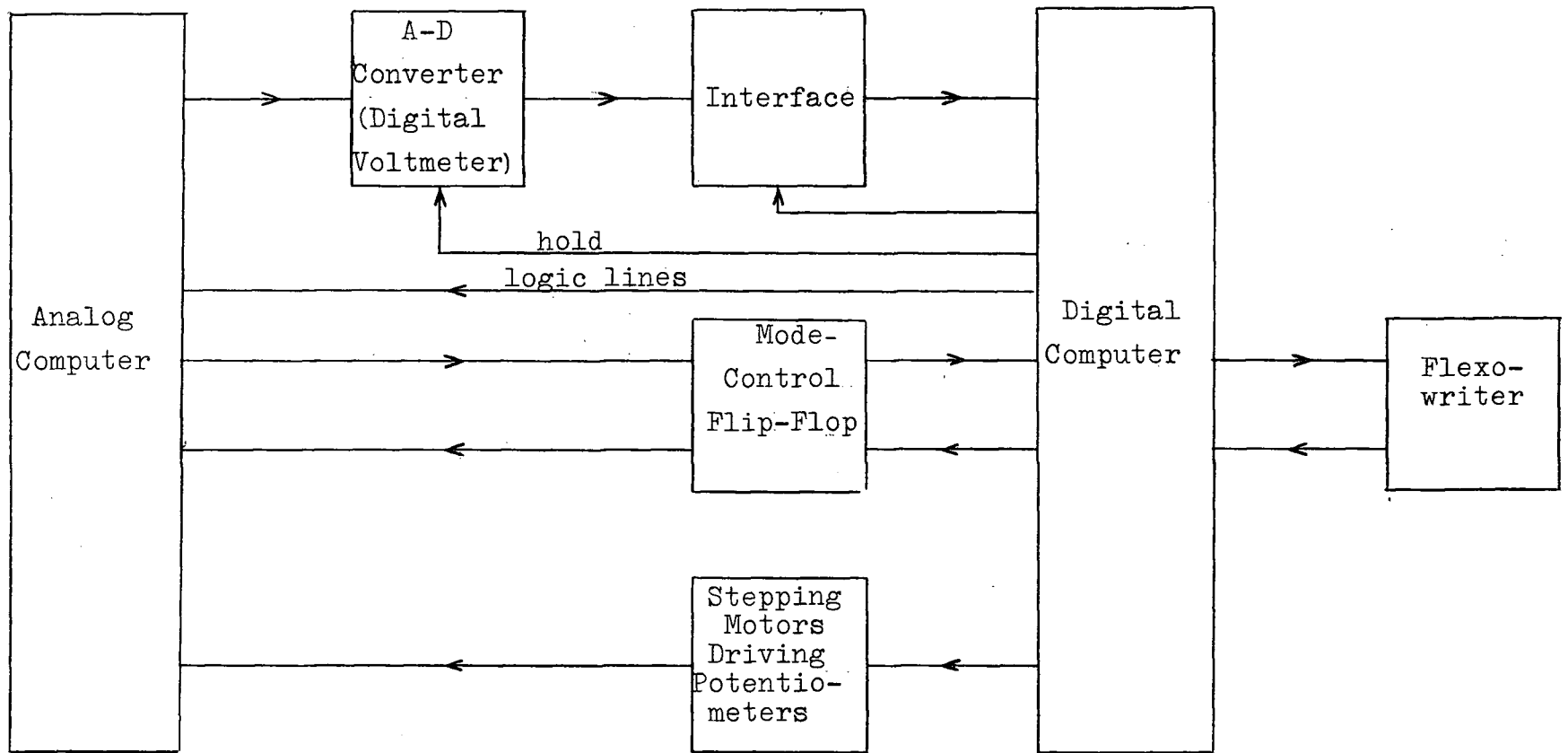


Figure 4-10. Hybrid Computer System

The interface, under control of the digital computer, transforms the binary-coded information to a form that is compatible with the input register of the digital computer. The entire procedure for the transfer of data from the analog computer to the digital computer is initiated, as has been described, by a signal from the mode-control flip-flop. The operation of the interface is described in Appendix I.

Digital-to-analog conversion is achieved by driving potentiometers with stepping motors. As explained in Appendix I, a prescribed number of pulses are sent to a stepping motor at a rate of 100 pulses/sec. to cause the wiper-arm voltage to change in accordance with the number of pulses transmitted. This rather slow, but economical, conversion scheme is adequate for the Monte Carlo methods since digital-to-analog conversion is required only for adjustment of the starting points (\bar{r}_0, t_0) after each set of N random walks.

The operation of the complete system is clarified by the detailed flow diagram (Figure 4-11) of a hybrid computer program used for the Monte Carlo methods. In terms of this flow diagram, the analog computer is equivalent to a subroutine for the generation of terminal values ϕ_i (or $\gamma_i \phi_i$). A machine-language program corresponding to the above flow diagram is given in Appendix IV.

The hybrid computer methods that have been outlined in this chapter are used in the following chapter to demonstrate the practicability of Monte Carlo methods for solving a large class of partial differential equations.

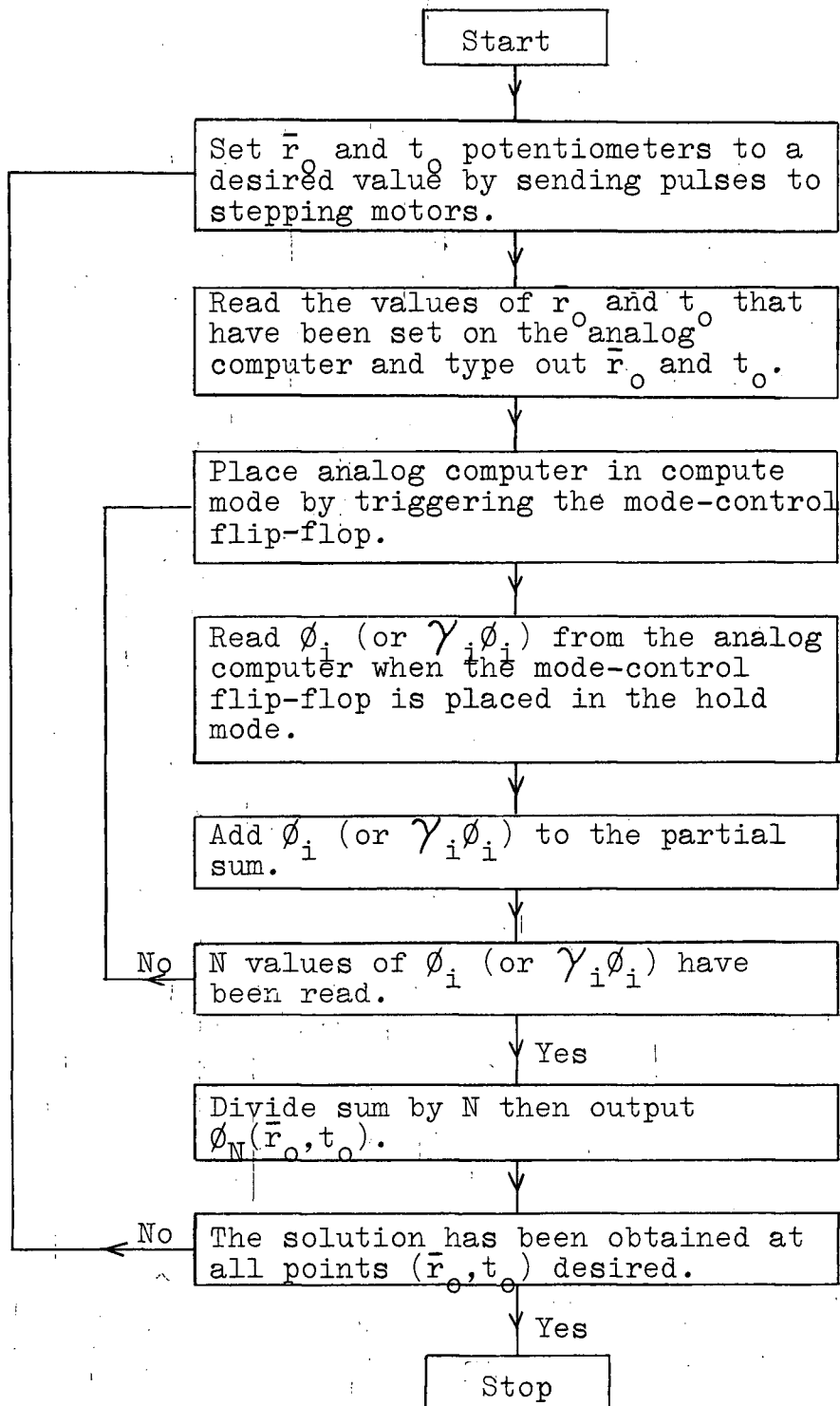


Figure 4-11. Flow Diagram for a Typical Hybrid Computer Program

5.1 Introduction

Hybrid computer solutions of a number of partial differential equations that were solved by Monte Carlo techniques are given in this chapter. The illustrative problems were chosen to substantiate the new methods that have been put forward as well as to indicate the type of results that can be expected from the Monte Carlo methods. The problems were also chosen so that exact analytical solutions could be found for comparison with the Monte Carlo solutions.

5.2 One-Dimensional Boundary-Value Problems

Three examples are given in this section. The first, which is actually a special case of the second, demonstrates a relationship between the duration of random walks and the power spectral density of the noise source. The second and third examples show, for various equation parameters and boundary conditions, that the Monte Carlo solutions are in close agreement with the exact solutions.

Example 1.

$$\frac{d^2\phi}{dx^2} = 0 \qquad \phi(-1) = -1$$

$$\qquad \qquad \qquad \phi(+1) = +1$$

The stochastic differential equation that must be simulated for this one-dimensional Laplace equation which is of type C (Section 3.3) is

$$\frac{dx}{dt} = N_1(t) .$$

Monte Carlo solutions of this problem are shown along the $\frac{K}{D_1} = 0$ line in Figure 5-1. To illustrate the variance of the Monte Carlo solutions, numerous solutions that were obtained at $x_0 = 0$

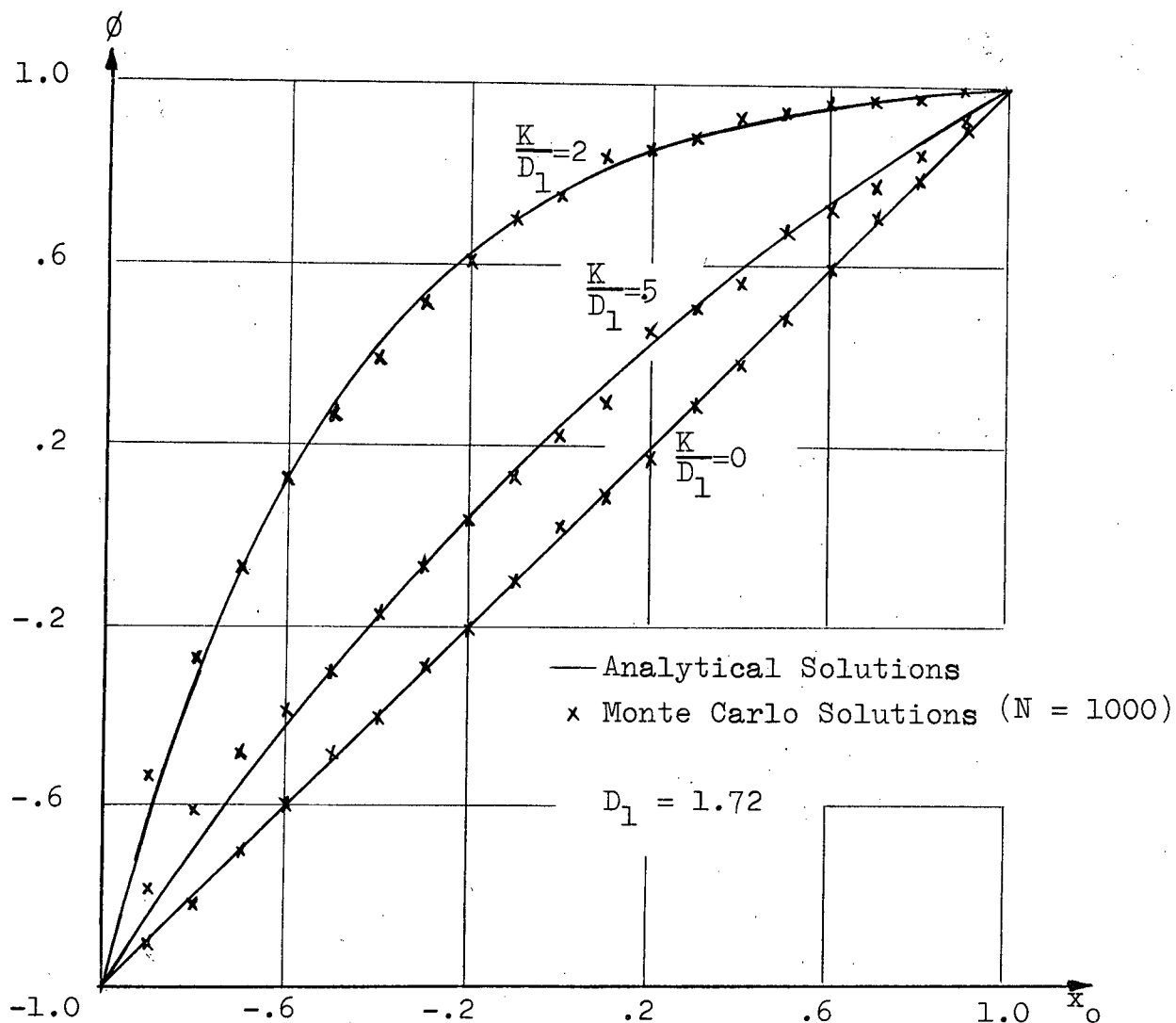


Figure 5-1. Solutions of $D_1 \frac{d^2 \phi}{dx_0^2} + K \frac{d\phi}{dx_0} = 0$.

are listed in Table 5-2. The largest deviation in this set of solutions is only 2.41% of the boundary values. Deviations of this order of magnitude are typical for solutions obtained with 1,000 random walks.

This problem, which is trivial to set up, is extremely useful for determining the power spectral density $2D_1$ of a noise source $N_1(t)$. As is shown in Appendix V, the average duration of a random walk starting at $x = x_0$ and terminating at $x = \pm 1$ is related to the power spectral density $2D_1$ through equation AV-10.

$$T(x_0) = \frac{1 - x_0^2}{2D_1}$$

Since $T(x_0)$, for any value of x_0 , is easily measured, D_1 can be determined. For this example the average duration $T(0)$ of random walks starting at $x_0 = 0$ was 290 ms. From this value

$$D_1 = \frac{1}{2T(0)} = 1.72 \text{ units}^2/\text{sec.}$$

where 1 unit \triangleq 100 volts.

0.21	1.61	0.61
-2.19	0.41	-0.59
0.81	-2.39	1.01
-0.79	-0.98	2.41
2.41	-0.99	-0.59
-1.39	-2.19	-0.79

Table 5-2. Values of $100 \phi_N(0)$ obtained with $N = 1000$.

As a check on the computer equipment and equation AV-10, a graph comparing theoretical values and two sets of measured values of $T(x_0)$, for $D_1 = 1.72$ units²/sec., was plotted. This graph is shown in Figure 5-3.

Since the above problem is extremely simple to set up and since the important parameter D_1 can be easily determined by measuring $T(0)$, it is often worthwhile to run this problem prior to more complex problems.

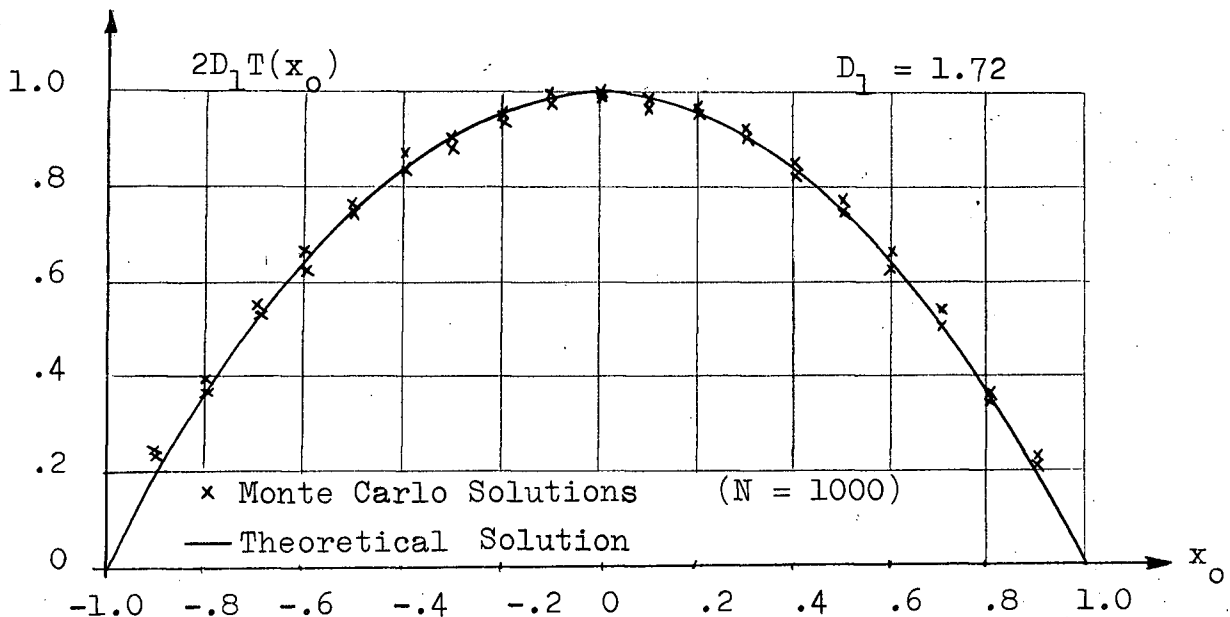


Figure 5-3. Average Time for a Random Walk used for the Solution of a One-Dimensional Laplace Equation.

Example 2.

$$D_1 \frac{d^2 \phi}{dx_0^2} + K \frac{d\phi}{dx_0} = 0 \quad \begin{array}{l} \phi(-1) = -1 \\ \phi(+1) = +1 \end{array}$$

The stochastic differential equation for this example of Problem C is

$$\frac{dx}{dt} - K = N_1(t).$$

Solution curves for

$$\frac{K}{D_1} = 0, 0.5 \text{ and } 2.0$$

with $D_1 = 1.72 \text{ unit}^2/\text{sec.}$ (from Example 1.) are shown in Figure 5-1.

Example 3.

$$\frac{d^2 \phi}{dx_0^2} - (1 - x_0^2)\phi = 0 \quad \begin{array}{l} \phi(-1) = -1 \\ \phi(+1) = A \end{array}$$

This is an example of Problem D, Section 3.3. The stochastic differential equation is

$$\frac{dx}{dt} = N_1(t)$$

and the related functional is $\gamma = \exp \left[-D_1 \int_{t_0}^{t_b} (1 - x^2) dt \right]$.

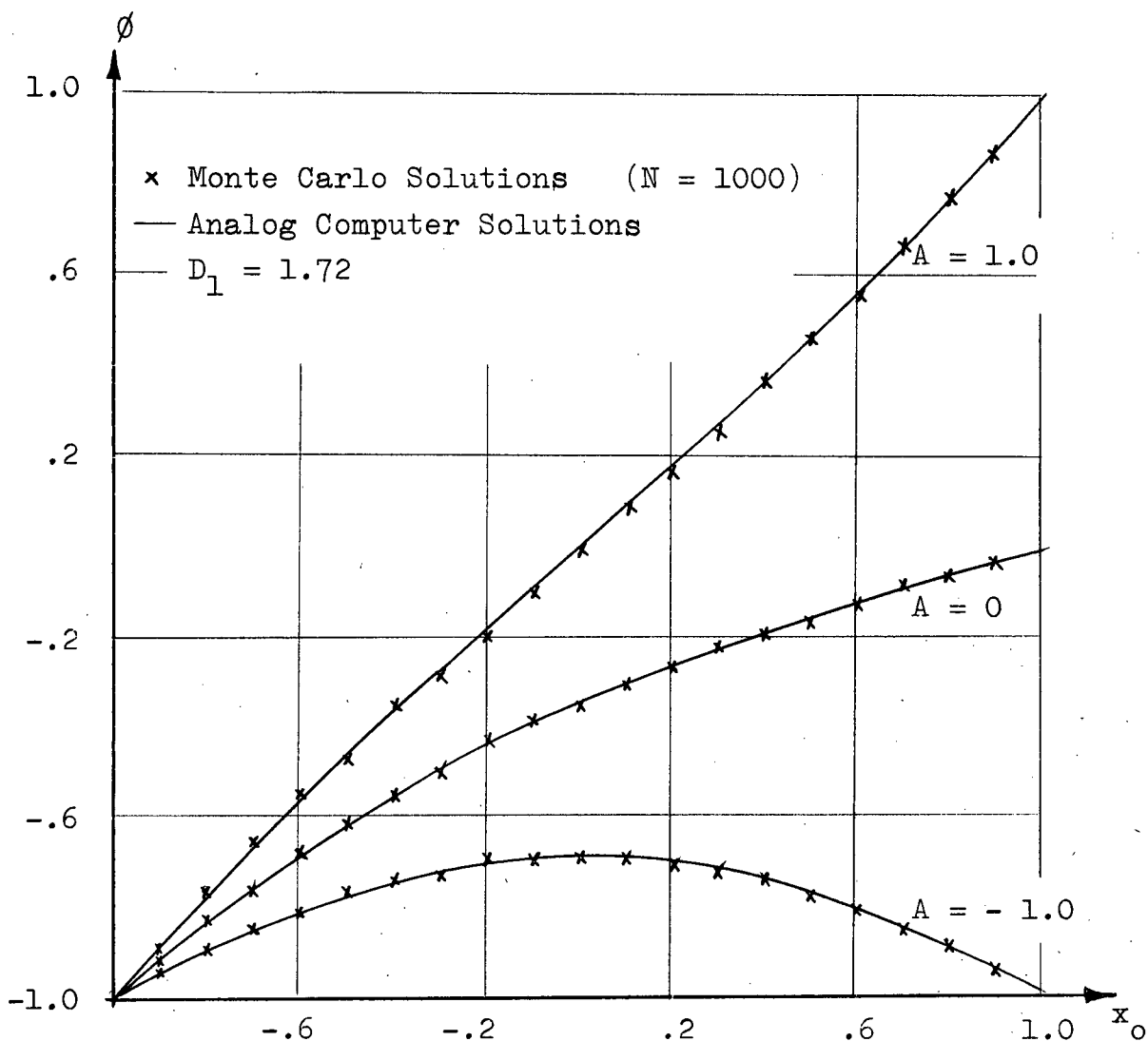


Figure 5-4. Solutions of $\frac{d^2 \phi}{dx_0^2} - (1 - x_0^2) \phi = 0$

The integral in the functional expression is scaled by D_1 since the noise source $N_1(t)$ has power spectral density $2D_1$ rather than 2 as implied by the problem equation. Two sets of Monte Carlo solutions, for three values of A , are compared with direct analog computer solutions in Figure 5-4.

5.3 Laplace's Equation in Two Dimensions

This example demonstrates that Monte Carlo methods are convenient for solving partial differential equations at a point. The potential ϕ at the point $x_0 = -.75$, $y_0 = 0$ of the region shown in the centre portion of Figure 5-5 is determined as a function of the centre position d of the inner circle. Monte Carlo solutions for 1,000 and 10,000 random walks per solution are shown in Figure 5-5. A time of approximately 2 minutes was required for each 1,000 walks. In this example the boundaries were detected by comparing $x^2 + y^2$ with 1 and $(x - d)^2 + y^2$ with $(.25)^2$. The centre position d of the inner circle was varied simply by adjusting a potentiometer.

5.4 Poisson's Equation in Two Dimensions

Poisson's equation, $\frac{\partial^2 \phi}{\partial x_0^2} + \frac{\partial^2 \phi}{\partial y_0^2} = 2$, is solved

with boundary condition $\phi_c = \frac{x_b^2}{2} + \frac{y_b^2}{2}$ on the boundary C of

region R (see insert in Figure 5-6). The boundary condition was chosen to satisfy the Poisson equation so that an exact solution

$$\phi = \frac{x_0^2}{2} + \frac{y_0^2}{2}$$

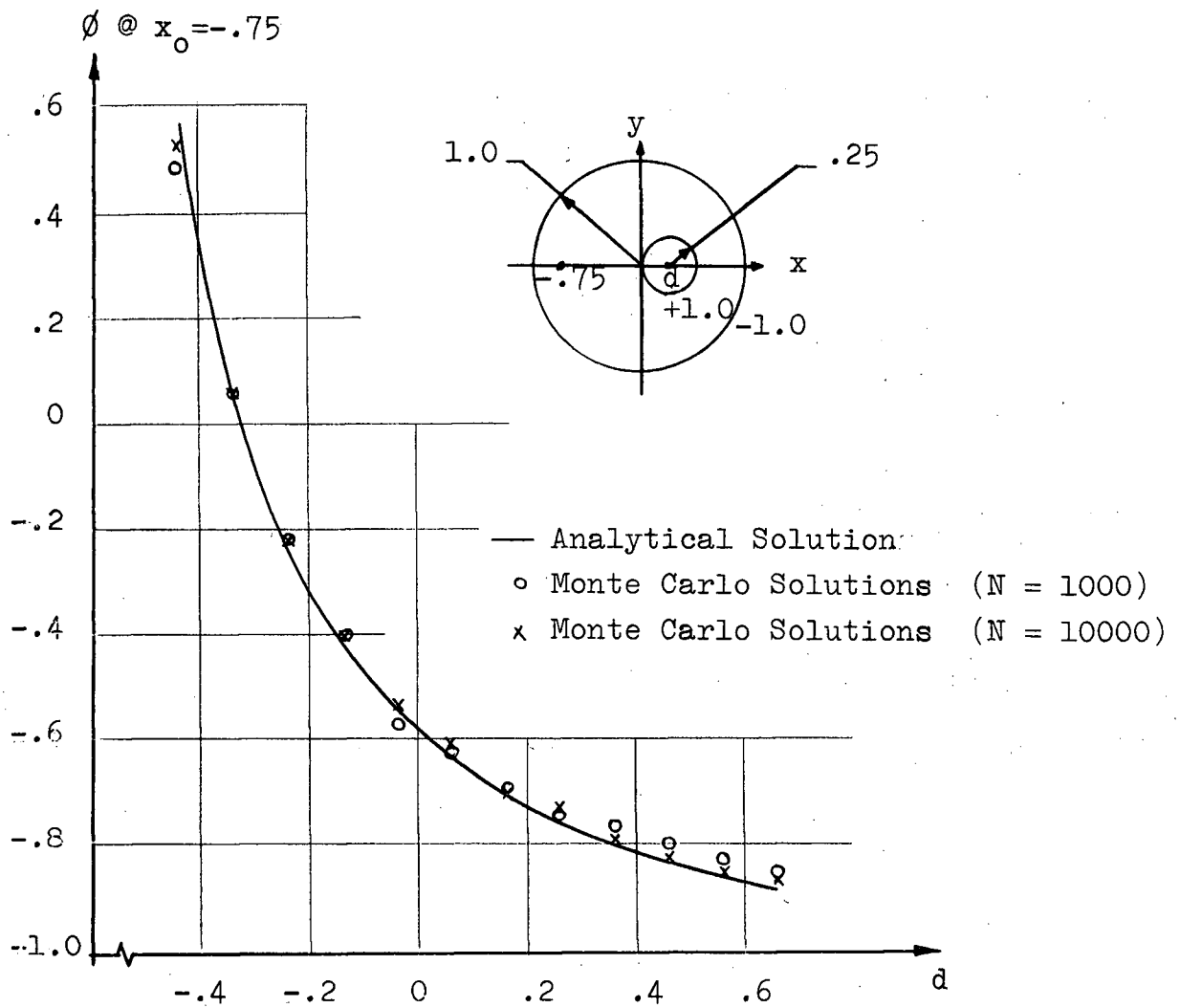


Figure 5-5. Solutions of Laplace's Equation as a Function of a Boundary Position.

could be found. For this choice of boundary condition the exact solution is actually independent of the shape of R . This, however, cannot be predicted by the computer so that no loss of generality results.

As outlined in Section 3.3, Problem E, the solution of this problem is given by

$$\phi(\bar{r}_0) = \phi_1(\bar{r}_0) + \int_{-\infty}^0 \phi_2(\bar{r}_0, t_0) dt_0 \quad (3.35)$$

where $\phi_1(\bar{r}_0)$, for this example, is the solution of Laplace's equation

$$\frac{\partial^2 \phi_1}{\partial x_0^2} + \frac{\partial^2 \phi_1}{\partial y_0^2} = 0$$

with boundary condition

$$\phi_c = \frac{x_b^2}{2} + \frac{y_b^2}{2} \quad \text{on } C \text{ of } R.$$

$\phi_2(\bar{r}_0, t_0)$ is the solution of the heat equation

$$-\frac{\partial \phi_2}{\partial t_0} = \frac{\partial^2 \phi_2}{\partial x_0^2} + \frac{\partial^2 \phi_2}{\partial y_0^2}$$

with initial condition

$$\phi_2(\bar{r}_0, 0) = -2$$

and zero boundary conditions on C of R .

The stochastic differential equations used for this example are

$$\frac{dx}{dt} = N_1(t)$$

$$\frac{dy}{dt} = N_2(t)$$

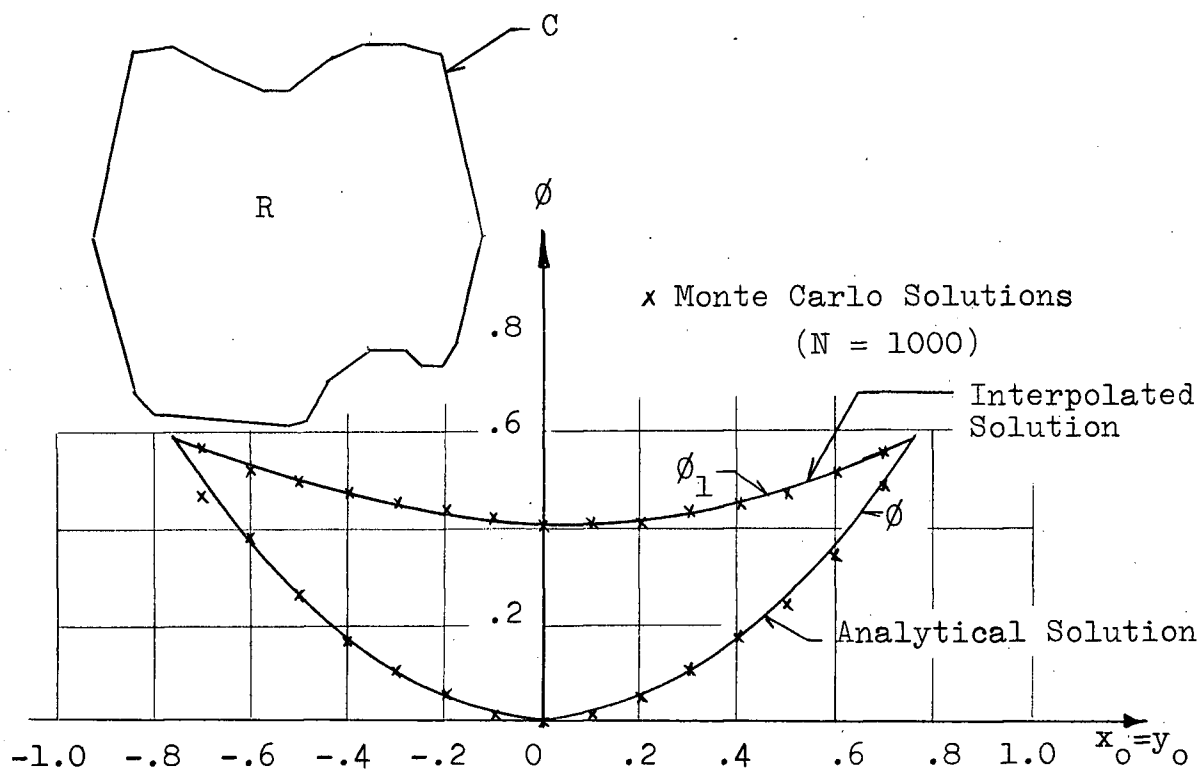


Figure 5-6. Solutions of Poisson's Equation and Laplace's Equation in the Region Shown.

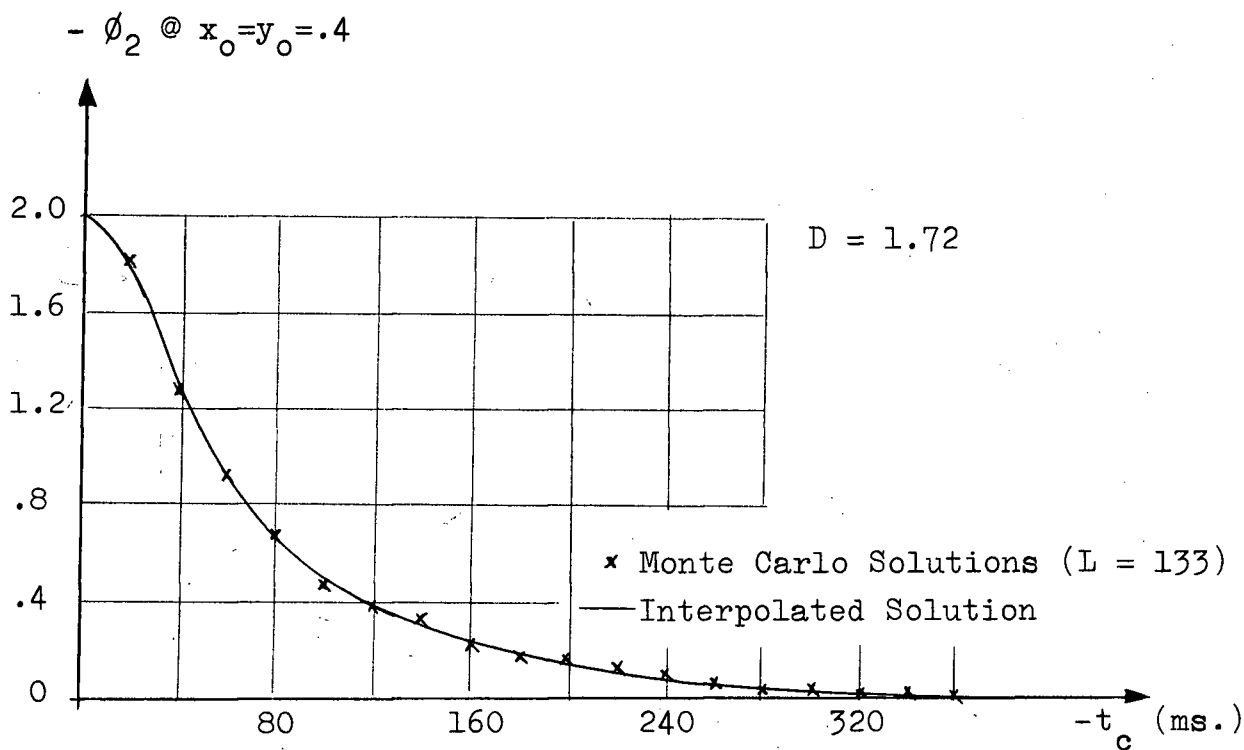


Figure 5-7. Solutions of the Heat Equation used in the Solution of Poisson's Equation.

with $D_1 = D_2 \triangleq D$. Since the function $\phi_2(\bar{r}_0, t_0)$ is a function of time, the computer time variable t_c must be scaled in accordance with D . The correct scaling is $t_0 = Dt_c$.

Monte Carlo solutions of $\phi(\bar{r}_0)$ along the line $x_0 = y_0$ are shown in Figure 5-6. The solution ϕ at $x_0 = y_0 = .4$, for example, is the sum of ϕ_1 at $x_0 = y_0 = .4$ and the integral with respect to t_0 of ϕ_2 at $x_0 = y_0 = .4$. As given in Figure 5-6, ϕ_1 at $x_0 = y_0 = .4$ is .44. The integral of ϕ_2 at $x_0 = y_0 = .4$, from a trapezoidal rule integration of the values of ϕ_2 given in Figure 5-7 is -.27. Hence, ϕ at $x_0 = y_0 = .4$ is

.44 - .27 = .17. This value is one of the values plotted in Figure 5-6.

For this problem, 1,000 random walks and 133 random walks were simulated for each value of ϕ_1 and ϕ_2 , respectively. These values, $N = 1,000$ and $L = 133$, were determined in accordance with the analysis of Section 3.5 C. The total solution time for each value of $\phi(\bar{r}_0)$ was approximately 12 minutes.

5.5 Heat Equation in One, Two and Three Dimensions

Solutions of the heat equation

$$-\frac{\partial \phi}{\partial t_0} = \nabla^2 \phi$$

with initial conditions $\phi_0(\bar{r}_0) = -1$, and boundary conditions $\phi_c(\bar{r}_b) = +1$, at the centre of a line, a square and a cubic region are shown in Figure 5-8. The three problems, which are examples of Problem A, Section 3.2, were solved using noise sources with $D = 1.72$ units²/sec. and using two, four or six electronic comparators to detect the boundaries. For these problems, it is important to note that the average time $T(0)$ for a random walk to reach a boundary decreases significantly with the dimension of the problem. In all cases $T(0)$ falls within the bounds established in Appendix V.

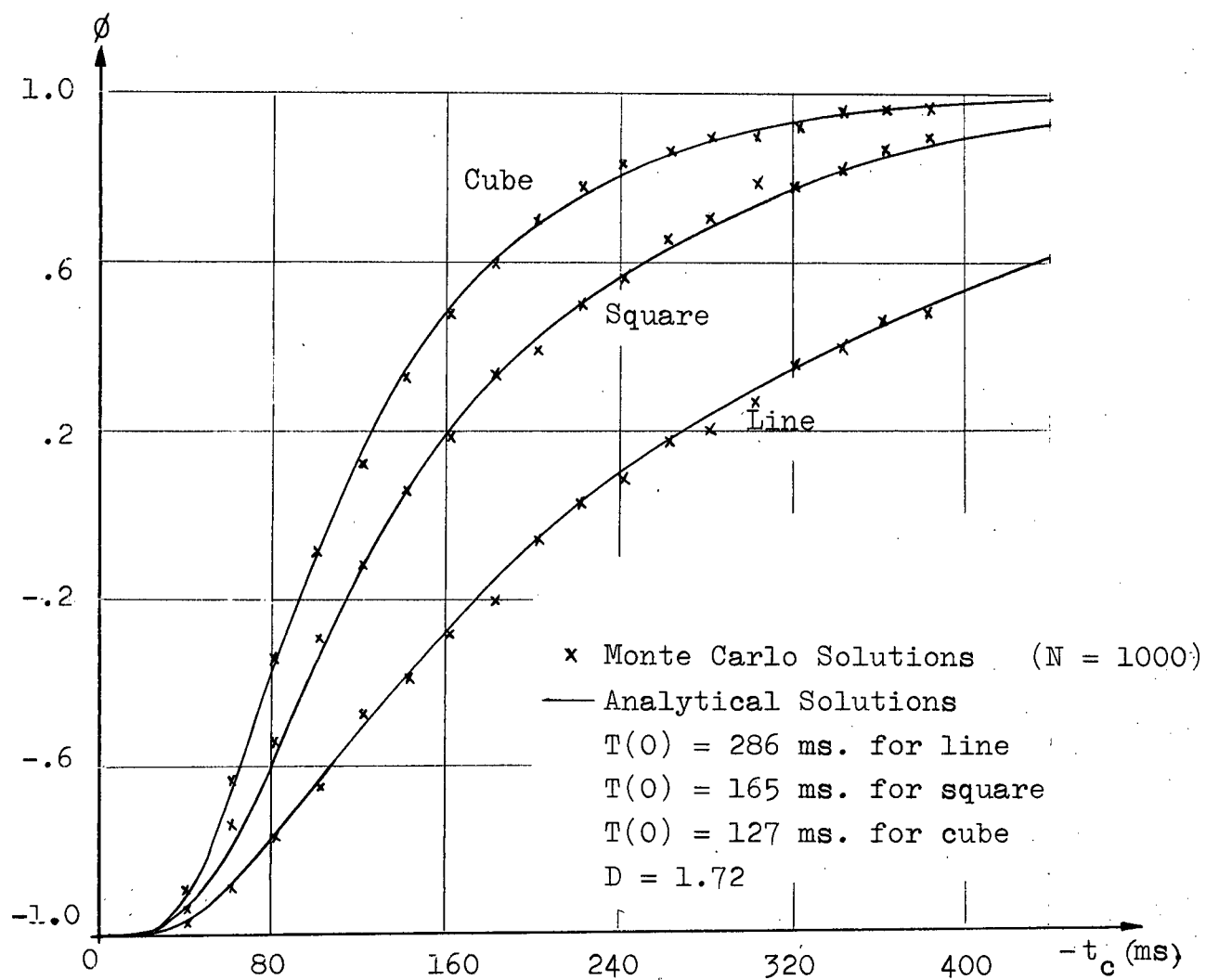


Figure 5-8. Solutions of the Heat Equation at the Centre of a Line, a Square and a Cubic Region.

5.6 Laplace's Equation in Three Dimensions

The final example is of Laplace's equation, $\nabla^2\phi = 0$, in the cubic region bounded by planes $x = \pm 1$, $y = \pm 1$, and $z = \pm 1$. Monte Carlo solutions along the line $x_0 = y_0 = z_0$ for the boundary condition

$$\phi_c(\bar{r}_b) = (x_b^2 - z_b^2) + (y_b^2 - z_b^2) + x_b y_b - y_b z_b + x_b z_b$$

are shown in Figure 5-9. The boundary condition was chosen to satisfy the Laplace equation so that the exact analytical solution is known for all x_0 , y_0 and z_0 .

For this example, six electronic comparators were used to detect the boundaries, and quarter-square multipliers were used to generate $\phi_c(\bar{r}_b)$. Approximately 5 minutes were required for each point solution.

5.7 Discussion of Results

In the examples given and in many other examples that were set up during this study, the Monte Carlo solutions were in close agreement with exact solutions. In all cases, good results were obtained in a straight-forward manner without the need of critical adjustments.

For most point solutions it was found that 1,000 random walks gave results satisfactory for verifying the methods. An average of about 5 minutes was required for each solution. This time with a fast analog computer (20 mc bandwidth) coupled to a fast digital computer could be reduced to about 1 sec.

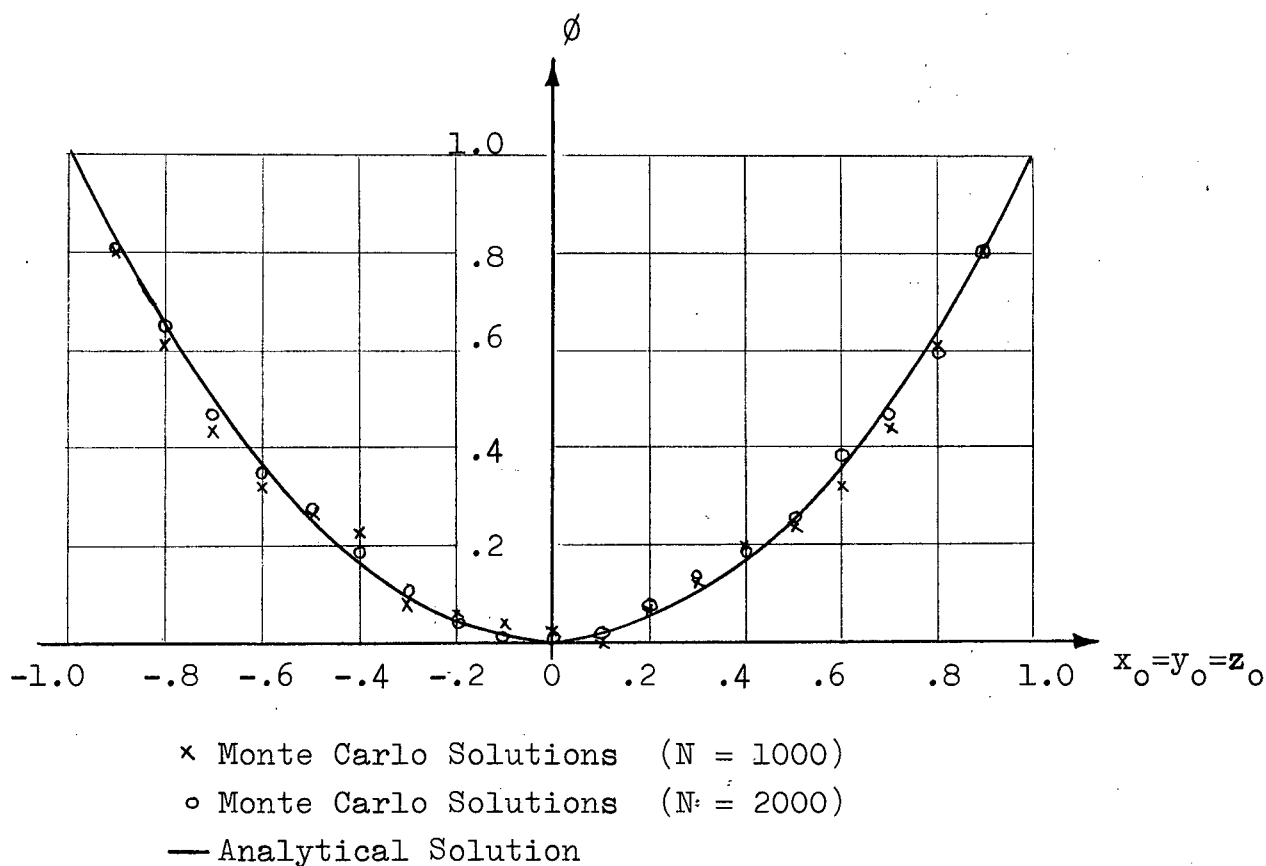


Figure 5-9. Solutions of Laplace's Equation in Three Dimensions.

Even with slow computers, however, Monte Carlo solutions at a few points can be obtained in about the same time that is required for finite-difference solutions on a fast digital computer. With finite-difference methods, however, solutions at many points are obtained simultaneously.

The ease with which boundary positions can be changed was demonstrated in the example of Section 5.3. Since the position and shape of regions, as well as boundary and initial values, can be altered very easily, it is suggested that this unique feature of the Monte Carlo methods could be used to

advantage in engineering design. For example, a Monte Carlo solution of a design problem in which a boundary or boundary value must be found to give a particular potential at a specified point could be solved easily. This type of problem on a digital computer, however, would require setting up a new finite-difference grid and solving for a complete set of potentials for each trial boundary or boundary value.

6. CONCLUSIONS

Monte Carlo methods have been developed for obtaining approximate solutions to homogeneous and nonhomogeneous elliptic, and homogeneous parabolic partial differential equations. Hence, equations of a much more general form than the class of homogeneous elliptic equations treated in the Michigan report⁴ can now be solved by Monte Carlo methods. Hybrid computer techniques for implementing the Monte Carlo methods have been proposed and tested. The techniques use to advantage the high-speed parallel operation of the analog computer as well as the memory and dynamic range of the digital computer. Problems are easy to program, and equation parameters, boundaries, and initial and boundary values are easily modified.

On the PACE-ALWAC hybrid system that was used to solve the example problems, 1,000 random walks could be simulated in about 5 minutes. With a fast hybrid system however, 1,000 random walks could be simulated in about 1 sec. In nearly all cases, the solutions that were obtained with 1,000 random walks were within 5% of the maximum initial or boundary value of the exact solutions. Thus, with 1,000 random walks, solutions with sufficient accuracy for many engineering problems are obtained in a reasonable time.

In the methods that have been developed, the solutions are obtained in a point-by-point manner. The solution at one point does not depend upon the solutions at neighboring points or upon the total number of solutions that are obtained. For

this reason the methods are particularly well suited to problems that require solutions at only a few points. If solutions at many points are required, finite-difference methods are more efficient.

The Monte Carlo methods that have been proposed require only a small hybrid computer whereas finite-difference methods for solving partial differential equations require either a large analog or a large digital computer. Hence, the Monte Carlo methods that have been developed seem ideal for small hybrid facilities where it would not be possible to employ other computing methods.

APPENDIX I

INTERFACE FOR TRANSFER OF DATA BETWEEN THE PACE 231 R-V
AND THE ALWAC III-E*

A block diagram of the interface for transfer of data from the PACE to the ALWAC is shown in Figure AI-1. The digital voltmeter (DVM) of the PACE is used for analog-to-digital conversion. The flip-flops that are shown in the figure are the input flip-flops of the ALWAC that are normally set from the flexowriter.

The value of an analog voltage is transferred from the PACE to the ALWAC in the following manner. The ALWAC is signaled, normally via the mode-control flip-flop, to read a value. The ALWAC supplies a "hold" signal to the DVM. About 30 ms. after the application of the hold signal a 5-digit plus sign binary-coded-decimal equivalent of the analog voltage is available at the DVM output. The sign and each decimal digit are transferred sequentially to the ALWAC flip-flops as follows. The ALWAC outputs a signal g_s which allows the sign from the DVM to enter FF4. This sign is then transferred to the ALWAC accumulator. The signal g_1 is then supplied. This allows the 10,000's digit (either a 0 or 1) to enter FF1 on its way to the accumulator. The ALWAC next outputs g_2 which allows the binary-coded 1,000's digit to enter flip-flops FF1, FF2, FF3 and FF4. The data is then transferred to the accumulator, and the process is continued until the 1's digit has been read. After all digits of the DVM have

* For a more detailed description of the interface, see reference (8).

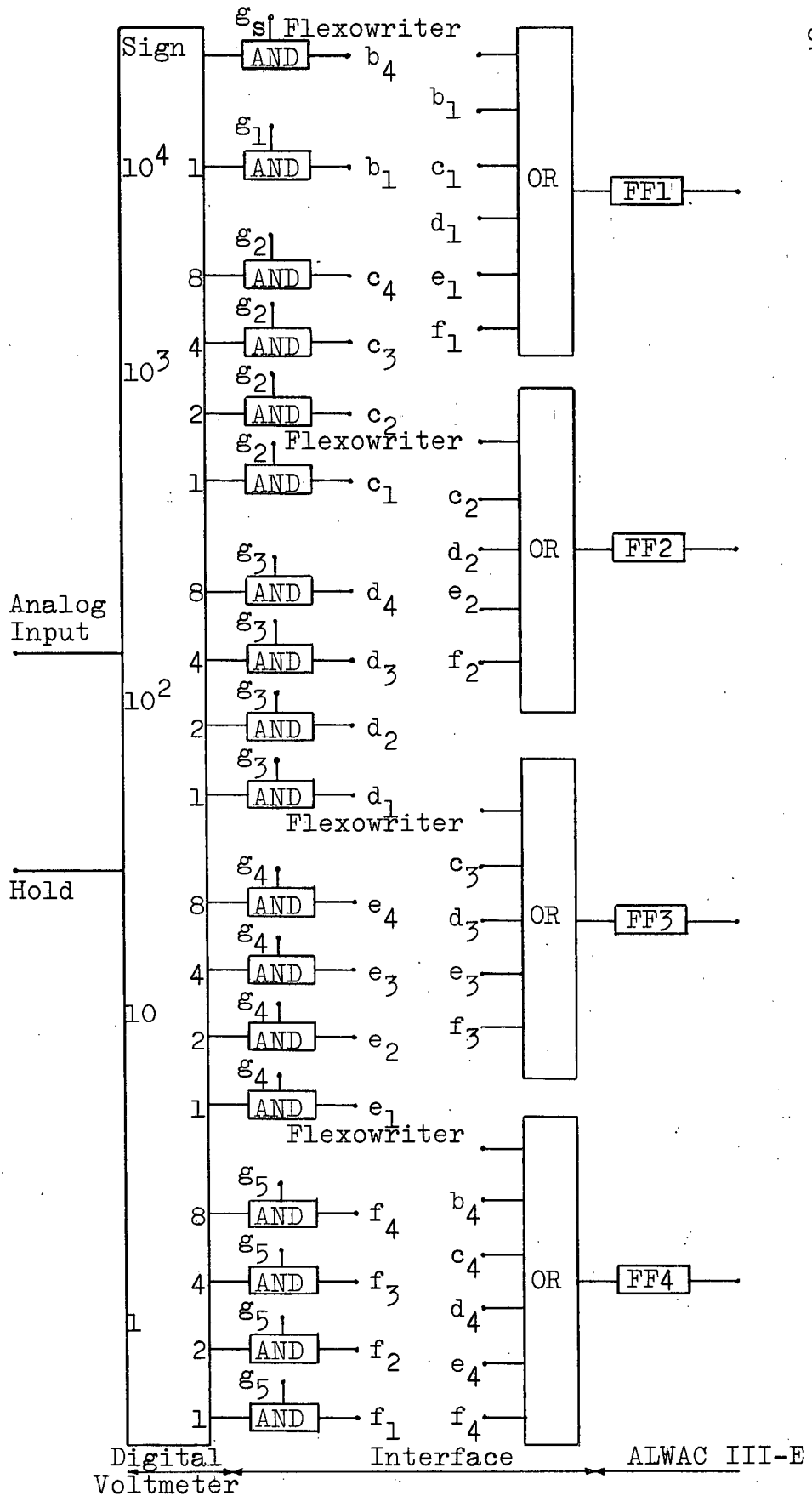


Figure AI-1. Interface for Transfer of Data Between PACE and ALWAC

been read into the accumulator, the "hold" is released by a signal from the ALWAC. The entire reading operation requires about 10 ms.

The analog voltage that is transferred to the ALWAC must be held at a constant value at least until the DVM has registered the correct number (~ 30 ms.). This is accomplished conveniently by an analog track-and-hold circuit that is controlled by the mode-control flip-flop (see Figure 4-10).

Data is transferred from the ALWAC to the PACE through potentiometers driven by stepping motors. The stepping motors are driven by pulses originating from dummy instructions in the ALWAC. A single pulse at one input of a stepping motor causes a $+15^\circ$ rotation while a pulse at the other input causes a -15° rotation. The motors are coupled to the potentiometers through 12-to-1 reduction gears. Therefore, if a 10-turn potentiometer has ± 100 volts across it, 144 pulses are required for a 10-volt change on the wiper arm. An example of a program to change the voltage on a wiper arm by 20 volts is shown in Figure AI-2. By this scheme, pulses can be sent to a stepping motor at a rate of approximately 100 pulses/sec.

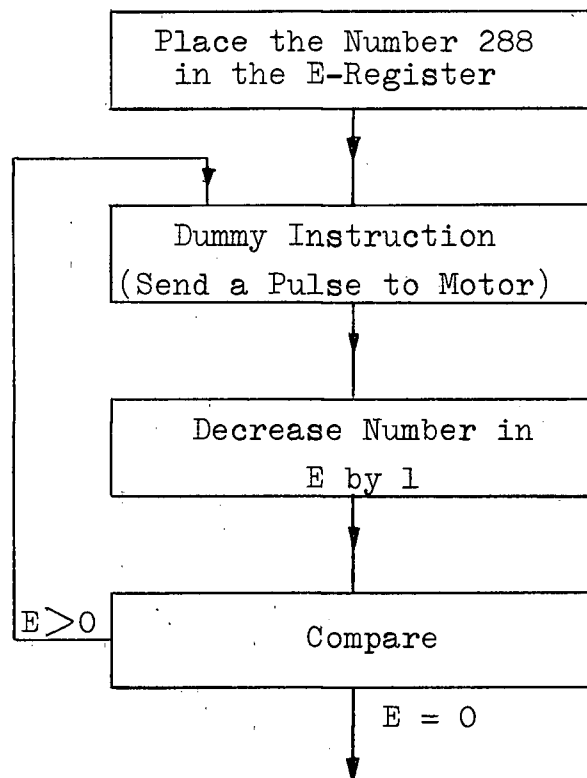


Figure AI-2. Instructions for Activating Stepping Motor

APPENDIX II

MULTICHANNEL DISCRETE-INTERVAL BINARY-NOISE SOURCE*

Numerous channels of stable, wide-band noise are required for Monte Carlo methods. A block diagram of an economical 3-channel noise source with these properties is shown in Figure AII-1. The Schmitt trigger is triggered at an average rate of "k" $0 \rightarrow 1$ state changes/sec. by the zero-crossings of the low-quality noise source. A sharp pulse from the ring counter is applied cyclically to each AND gate at a rate of f_c pulses/sec. If $k \gg f_c$, the outputs $N_1(t)$, $N_2(t)$ and $N_3(t)$ are essentially uncorrelated and the autocorrelation function of each channel is essentially zero for $|\tau| > \frac{1}{f_c}$

For output levels $\pm E$ volts, the autocorrelation function is

$$\begin{aligned} \phi(\tau) &= E^2 (1 - f_c |\tau|) & |\tau| &\leq \frac{1}{f_c} \\ &= 0 & |\tau| &> \frac{1}{f_c} \end{aligned} \quad (\text{AII.1})$$

The power spectral density $\Phi(\omega)$ corresponding to this autocorrelation function is

$$\Phi(\omega) = 2f_c E^2 \left[\frac{1 - \cos\left(\frac{\omega}{f_c}\right)}{\omega^2} \right] \quad (\text{AII.2})$$

* For a more detailed analysis of this noise source see reference (9)

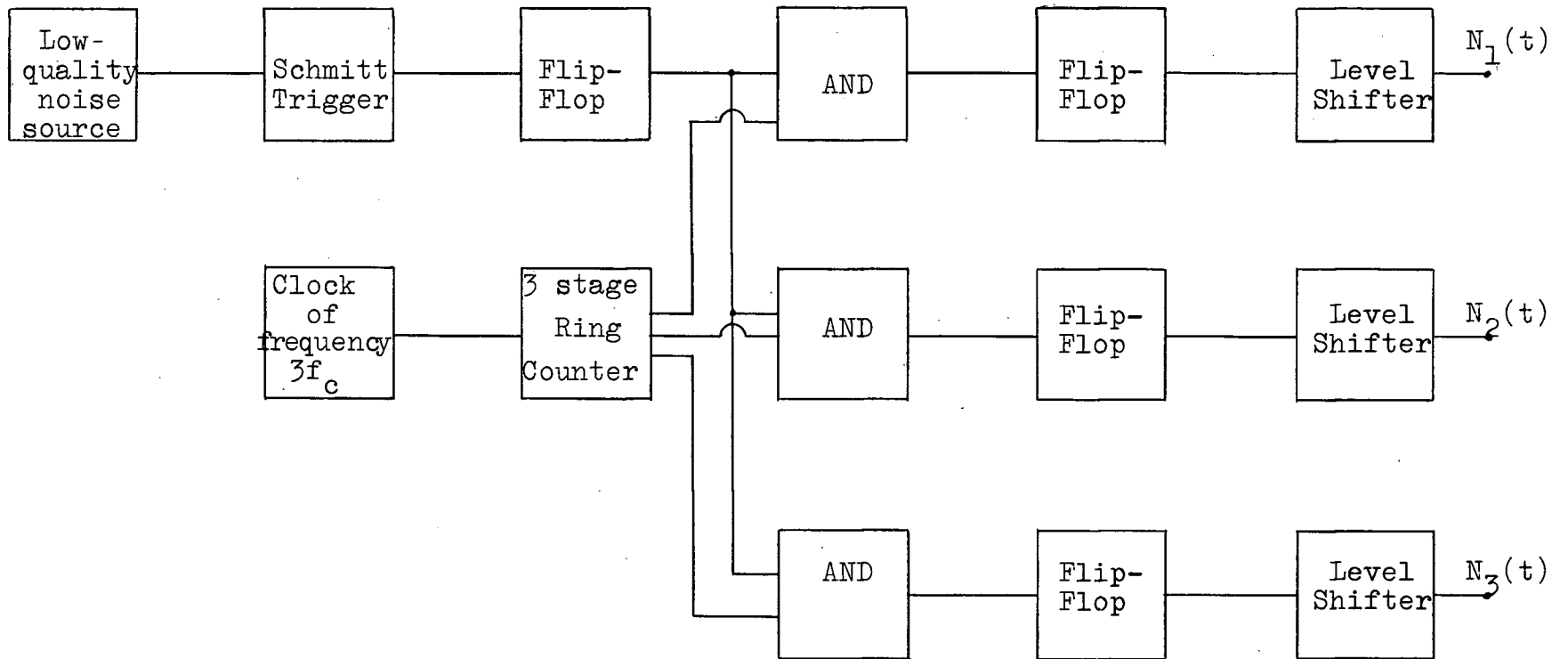


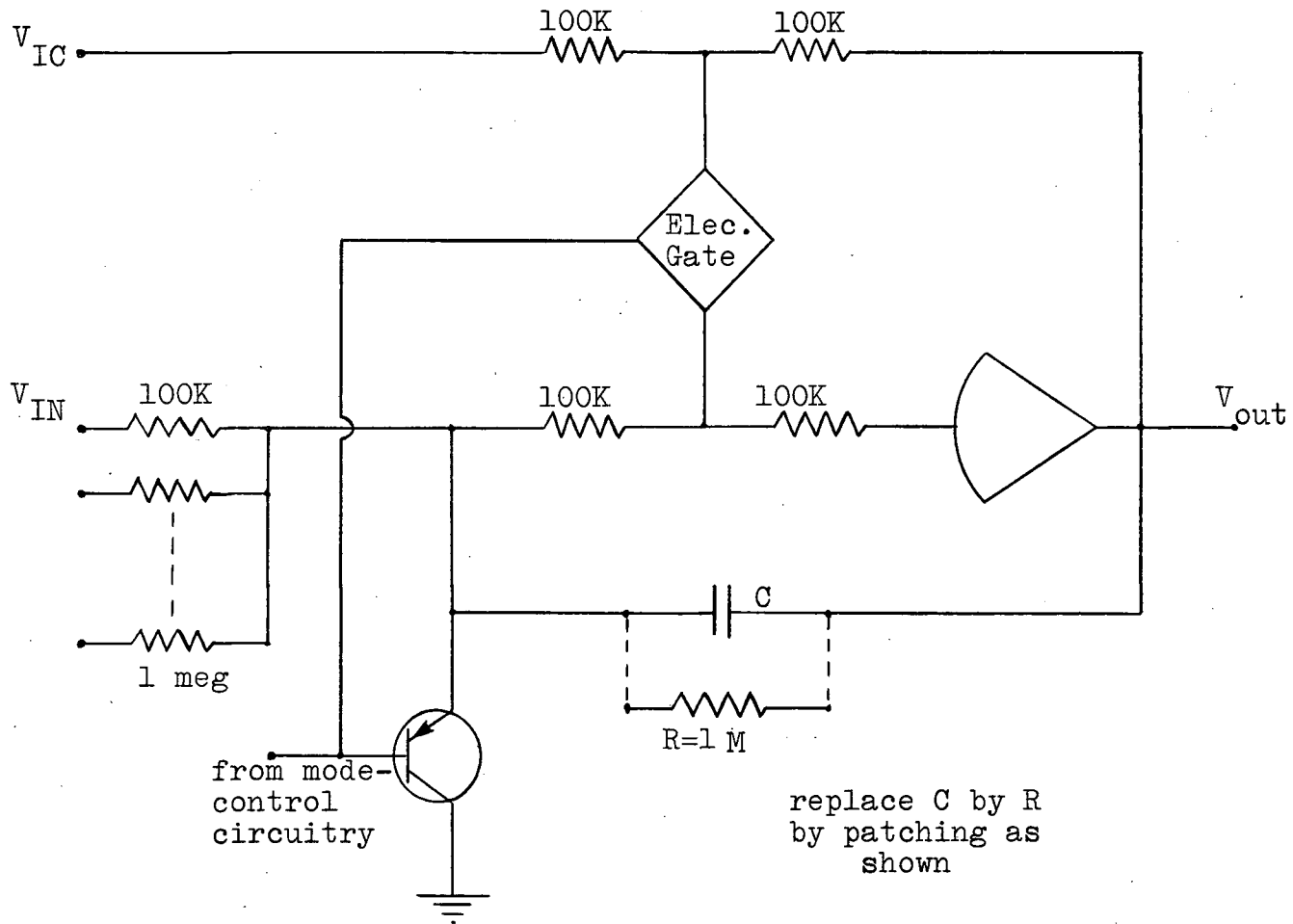
Figure AII-1. Block Diagram of 3-Channel Noise Source.

The Monte Carlo solutions given in Chapter 5 were obtained with $k = .4$ mc/sec., $f_c = 20$ kc/sec. and $E = 5$ volts. With these values the criterion $k \gg f_c$ is met, and the bandwidth of the noise channels is greater than the bandwidth capabilities of the analog computer.

APPENDIX III
AN ELECTRONIC SPDT SWITCH

By suitably patching a PACE 231 R-V amplifier equipped with electronic switching, a fast SPDT switch can be realized. The required patching is accomplished by placement of bottle plugs as shown in Figure AIII-1. This patching replaces the feedback capacitor C with a 1 M ohm resistor R and allows the output V_{out} to be switched between $-V_{\text{IC}}$ and $-V_{\text{IN}}$ under control on the mode-control signal c . When $c = +5$ volts, transistor T_1 and the electronic gate conduct so that $V_{\text{out}} = -V_{\text{IC}}$. When $c = 0$ volts, transistor T_1 and the electronic gate are open. In this mode $V_{\text{out}} = -V_{\text{IN}}$.

For $V_{\text{IC}} = +100$ volts and $V_{\text{IN}} = -100$ volts, the output V_{out} will switch from $-V_{\text{IC}}$ to $-V_{\text{IN}}$ in $160 \mu\text{sec.}$ and from $-V_{\text{IN}}$ to $-V_{\text{IC}}$ in $100 \mu\text{sec.}$



IC	PS
○	○
Coil	Coil
○	○
F	O
○	○

--- connections made by bottle plugs

replace C by R by patching as shown

Figure AIII-1. Circuit and Patching for a SPDT Switch

APPENDIX IV

A PROGRAM FOR IMPLEMENTING MONTE CARLO METHODS.

An ALWAC III-E program that carries out operations similar to those indicated in the flow diagram of Figure 4-11, Section 4.5 is given below:

b4 1

```

00|83b5 570f|80 01|4917 fff0|81 02|df00 d903|82 03|0001 0000|83
04|ffa0 1704|84 05|f9e0 f9e0|85 06|d10c dfda|86 07|03e8 0000|87
08|5703 118c|88 09|fle5 fff0|89 0a|1b08 2800|8a 0b|0000 0013|8b
0c|5705 2800|8c 0d|ffe0 1320|8d 0e|6d8b 2400|8e 0f|0090 0000|8f
10|4913 4917|90 11|4913 1714|91 12|4d8b 1980|92 13|0000 0000|93
14|f9e0 fff0|94 15|6117 0e00|95 16|1116 0000|96 17|0000 0000|97
18|7913 fff0|98 19|eb1b 3200|99 1a|0000 0000|9a 1b|05f5 e100|9b
1c|6117 fff0|9c 1d|d580 f5c8|9d 1e|0000 0000|9e 1f|0000 0000|9f
8fb649be

```

Immediately after the program is initiated, 144 pulses (contents of 0f) are sent to a stepping motor for adjustment of \bar{r}_0 . A multiplex signal (flag #1) allows the value of \bar{r}_0 to be read. Immediately after \bar{r}_0 is read, it is typed out. One thousand numbers (contents of 07) are then read from a fixed terminal of the analog computer upon signals from the mode-control flip-flop. These numbers are added to a partial sum as they are read. After the 1,000 numbers have been read and added together, the sum is typed out. Another 144 pulses are then sent to the stepping motor, and the process is repeated. The process is repeated a total of 19 times (contents of 8b).

APPENDIX V

AVERAGE DURATION OF RANDOM WALKS

In this appendix a partial differential equation is derived for the average time $T(\bar{r}_0)$ that is required for a random walk starting at \bar{r}_0 to reach a boundary for the first time. The equation is solved for special cases to give the average duration of a random walk that is used for the solution of Laplace's equation in a one, a two and a three-dimensional generalized spherical region. The approach that is used is similar to, but not as involved as, the method of Wasow for calculating the mean duration of discrete random walks.¹⁶

From the definition of $g(\bar{r}_b, t_b | \bar{r}_0, t_0)$ and from Chapman-Kolmogorov equation (2.2) it follows that

$$\int_C g(\bar{r}_b, t_b | \bar{r}_0, t_0) dr_b = \int_R \int_C g(\bar{r}_b, t_b | \bar{r}_1, t_1) dr_b f(\bar{r}_1, t_1 | \bar{r}_0, t_0) dr_1 \quad (\text{AV.1})$$

is the probability density for a random walk to reach a boundary for the first time at t_b if it started at (\bar{r}_0, t_0) . The average duration of a random walk starting at (\bar{r}_0, t_0) is therefore given by

$$\begin{aligned} T(\bar{r}_0, t_0) &= \int_{-\infty}^{\infty} (t_b - t_0) \int_C g(\bar{r}_b, t_b | \bar{r}_0, t_0) dr_b dt_b \\ &= \int_R \int_{-\infty}^{\infty} (t_b - t_0) \int_C g(\bar{r}_b, t_b | \bar{r}_1, t_1) dr_b dt_b f(\bar{r}_1, t_1 | \bar{r}_0, t_0) dr_1 \end{aligned} \quad (\text{AV.2})$$

$$\begin{aligned}
&= \int_{R-\infty}^{\infty} \int_{-\infty}^{\infty} (t_b - t_1) \int_C g(\bar{r}_b, t_b | \bar{r}_1, t_1) dr_b dt_b f(\bar{r}_1, t_1 | \bar{r}_0, t_0) dr_1 \\
&+ \int_{R-\infty}^{\infty} \int_{-\infty}^{\infty} (t_1 - t_0) \int_C g(\bar{r}_b, t_b | \bar{r}_1, t_1) dr_b dt_b f(\bar{r}_1, t_1 | \bar{r}_0, t_0) dr_1
\end{aligned}
\tag{AV.3}$$

Therefore,

$$\begin{aligned}
T(\bar{r}_0, t_0) &= \int_R T(\bar{r}_1, t_1) f(\bar{r}_1, t_1 | \bar{r}_0, t_0) dr_1 \\
&+ (t_1 - t_0) \int_R f(\bar{r}_1, t_1 | \bar{r}_0, t_0) dr_1
\end{aligned}
\tag{AV.4}$$

The last term follows from the fact that

$$\int_{-\infty}^{\infty} \int_C g(\bar{r}_b, t_b | \bar{r}_1, t_1) dr_b dt_b = 1
\tag{AV.5}$$

for random walks that are certain to terminate at a boundary.

Now let $t_1 = t_0 + \Delta t$ and expand $T(\bar{r}_1, t_0 + \Delta t)$ in a Taylor series about \bar{r}_0 in the same manner that was done in Chapter 2. If this is done and equation (2.9) and the limits (2.11) to (2.21) are used, it follows that

$$-\frac{\partial T}{\partial t_0}(\bar{r}_0, t_0) = L_{\bar{r}_0, t_0} T(\bar{r}_0, t_0) + 1
\tag{AV.6}$$

If the operator $L_{\bar{r}_0, t_0}$ is independent of t_0 , then $T(\bar{r}_0, t_0)$ is also independent of t_0 . For this case $T(\bar{r}_0, t_0)$ can be denoted by $T(\bar{r}_0)$ and

$$L_{\bar{r}_0} T(\bar{r}_0) + 1 = 0 \quad (\text{AV.7})$$

The boundary condition for $T(\bar{r}_0)$ is $T(\bar{r}_b) = 0$

If $L_{\bar{r}_0}$ is the operator that is used for the solution of Laplace's equation, then

$$D \nabla^2 T(\bar{r}_0) + 1 = 0 \quad (\text{AV.8})$$

For an n-dimensional generalized sphere of radius "a", $T(\bar{r}_0)$ depends only upon $r_0 = |\bar{r}_0|$, therefore,

$$D \frac{1}{r_0^{n-1}} \frac{d}{dr_0} \left[r_0^{n-1} \frac{dT(r_0)}{dr_0} \right] + 1 = 0$$

$$T(a) = 0 \quad (\text{AV.9})$$

The solution of the problem given by (AV.9) is

$$T(r_0) = \frac{a^2 - r_0^2}{2nD} \quad (\text{AV.10})$$

This result shows explicitly how the duration of a random walk depends upon the starting radius r_0 and the dimension of the sphere. By enclosing any other shape of region with a generalized spherical region, an upper bound on the average duration of

a random walk can be obtained. A lower bound can be obtained by enclosing a generalized spherical region by the region for which the lower bound is desired. For example, the average duration $T(0)$ of a random walk starting at the centre of a square region with sides $2a$ is

$$\frac{a^2}{4D} < T(0) < \frac{2a^2}{4D} \quad (\text{AV.11})$$

The average duration $T(0)$ of a random walk starting at the centre of a cubic region with edges $2a$ is

$$\frac{a^2}{6D} < T(0) < \frac{3a^2}{6D} \quad (\text{AV.12})$$

REFERENCES

1. Forsythe, G.E., and Wasow, W.R., Finite-Difference Methods for Partial Differential Equations, John Wiley and Sons Inc., New York, 1960.
2. Curtiss, T.J.H., "Sampling Methods Applied to Differential and Difference Equations", Proc. Seminar on Scientific Computation, International Business Machines Corp., New York, N.Y., November 1949.
3. Meyer, Herbert A., Editor, Symposium on Monte Carlo Methods, John Wiley and Sons Inc., New York, 1956.
4. Chuang, K., Kazda, L.F., and Windeknecht, T., "A Stochastic Method of Solving Partial Differential Equations using an Electronic Analog Computer", Project Michigan Report 2900-91-T, Willow Run Laboratories, University of Michigan, June 1960.
5. MacKay, D.M., and Fisher, M.E., Analogue Computing at Ultra-High Speed, Chapter 16, John Wiley and Sons Inc., New York, 1962.
6. Karplus, Walter J., Analog Simulation, McGraw Hill Book Company, Inc., New York, 1958.
7. Middleton, David, Statistical Communication Theory, Chapters 1 and 10, McGraw Hill Book Company, Inc., New York, 1960.
8. Soudack, A.C., and Little, W.D., "An Economical Hybridizing Scheme for Applying Monte Carlo Methods to the Solution of Partial Differential Equations", Simulation, Vol. 5, No. 1, pp. 9-11, July, 1965.
9. Kohne, H., Little, W.D., Soudack, A.C., "An Economical Multichannel Noise Source", Simulation, Vol. 5, No. 8, November, 1965.
10. Bharucha-Reid, A.T., Elements of the Theory of Markov Processes and their Applications, Chapter 3, McGraw Hill Book Company, Inc., New York, 1960.
11. Wang, Ming Chen, and Uhlenbeck, G.E., "On the Theory of Brownian Motion II", Reviews of Modern Physics, Vol. 17, Nos. 2 and 3, pp. 323 - 342, April - July 1945.
12. Darling, D.A., and Siegert, A.J., "A Systematic Approach to a Class of Problems in the Theory of Noise and Other Random Phenomena, Part I", IRE Trans. on Information Theory, Vol. IT-3, pp. 32 -37, March, 1957.

13. Wilkinson, R.H., "A Method of Generating Functions of Several Variables using Analog Diode Logic", IEEE Trans. On Electronic Computers, Vol. EC-12, pp. 112-129, April, 1963.
14. Hampton, R.L.T., "A Hybrid Analog-Digital Pseudo Random Noise Generator", Simulation, Vol. 4, No. 3, pp. 179-185, March, 1965.
15. Tomovic, R., and Karplus, W., High-speed Analog Computers, Chapter 5, John Wiley and Sons Inc., New York, 1962.
16. Wasow, Wolfgang, "On the Mean Duration of Random Walks", Journal of Research of the National Bureau of Standards, Vol. 46, No. 6, pp. 462 - 471, June, 1951.

Addendum

Since the preparation of this thesis, the following books have been brought to the author's attention:

Dynkin, E.B., Markov Processes, Vol. I and Vol. II, Academic Press Inc. Publishers., New York, 1965.

These books contain an extensive treatment of Markov processes. In particular, Chapter 13 of Volume II has a theoretical discussion of problems similar to those discussed in Section 3.3 of this thesis.